Title
The Cellular Logic of Pain Modality Discrimination

Author
Cavanaugh, Daniel

Publication Date
2009

Peer reviewed|Thesis/dissertation

The Cellular Logic of Pain Modality Discrimination

by

Daniel J. Cavanaugh

DISSERTATION

Submitted in partial satisfaction of the requirements for the degree of

DOCTOR OF PHILOSOPHY

in

Neuroscience

in the

GRADUATE DIVISION

of the

UNIVERSITY OF CALIFORNIA, SAN FRANCISCO

The Cellular Logic of Pain Modality Discrimination

Daniel J. Cavanaugh

Abstract

Noxious stimuli are detected by primary afferent neurons of the dorsal root ganglia (DRG). Such neurons, known as nociceptors, can be divided into several distinct populations based on the heterogeneous distribution of receptors, ion channels, and neurotransmitters, however, functional correlates of these anatomical differences are yet unidentified. The work in this thesis further examines the neurochemical and functional segregation of nociceptor subtypes through a genetic and pharmacological investigation of neurons that express the heat and capsaicin receptor, TRPV1.

TRPV1 is activated by noxious heat stimuli (>43 ^{o}C), and is robustly expressed by primary afferent nociceptors. In addition, some have argued that TRPV1 is widely distributed in cells outside of the DRG, although there is considerable disagreement as to the extent and localization of this expression. To address this question, we generated a line of mice in which TRPV1^{+} cells co-express two reporter genes: placental alkaline phosphatase and nuclear lacZ. These enzymes allow for the sensitive and accurate identification of TRPV1^{+} cells and processes. Using this approach, we observed that, in contrast to numerous previous reports, TRPV1 expression in the nervous system is largely limited to peptidergic, primary afferent neurons. We additionally found evidence for TRPV1

in arteriolar smooth muscle cells, highlighting an important substrate for the actions of heat, protons, and other TRPV1 agonists on vascular tone.

We then investigated the relative contribution of $TRPV1^+$ and $TRPV1^-$ nociceptors to the behavioral responses to stimuli of different pain modalities. Surprisingly, despite the fact that most nociceptors show polymodal response properties in electrophysiological assays, we found that pharmacological ablation of the central branches of $TRPV1^+$ nociceptors selectively abolished heat pain sensitivity without altering behavioral responses to mechanical or cold stimuli. Conversely, we found that genetic ablation of nociceptors expressing the G protein-coupled receptor, MrgprD, which marks a large subset of $TRPV1^-$ DRG neurons, selectively reduced behavioral sensitivity to noxious mechanical stimuli. This double-dissociation suggests that the brain can distinguish different noxious stimulus modalities from the earliest stages of sensory processing as a result of distinct contributions from molecularly-defined nociceptor subtypes.

Table of Contents

Chapter 1

Introduction to pain and the primary afferent nociceptor

Pain is an unpleasant sensory or emotional experience that results from real or perceived tissue damage (Loeser and Treede, 2008). As a conscious perception, pain is distinguished from nociception, which is the transduction of noxious stimuli by primary afferent neurons in the pain system (Loeser and Treede, 2008). The process of nociception thus underlies pain perception, but the pain experience results from cognitive and emotional processing of nociceptive signals by the brain (Fields, 2004).

Historically, two conflicting views were proposed as to the experience of pain and its mechanisms. One view held that pain resulted from the distributed activation of nonspecialized somatosensory neurons. In this view, the central nervous system (CNS) interpreted sensory activation as pain if that activation reached a certain magnitude and distribution (Craig, 2003; Perl, 2007). Others posited that pain sensation was mediated by the activation of specific “pain” fibers, which could only be activated by stimuli of sufficient threshold, in the noxious range (Craig, 2003; Perl, 2007). This idea of a specialized “pain” system was first popularized in the early 20th century by von Frey and Sherrington, among others, but it wasn’t until the 1960s, when the development of modern electrophysiological methods allowed for the unequivocal identification of

nociceptive-specific primary afferent neurons (known as nociceptors), that the specificity argument became generally accepted as the de facto organization of somatosensation (Woolf and Ma, 2007; Perl, 2007).

More recently, the application of molecular biological techniques to the study of pain has demonstrated that the ability to detect and respond to certain external stimuli requires the presence of specific molecular transducers, and anatomical analysis has revealed that these molecules show a differential distribution among classes of primary somatosensory neurons (Julius and Basbaum, 2001; Woolf and Ma, 2007). Further, these classes exhibit differences in developmental timecourse, dependence on neurotrophic factors for survival, and in the CNS circuits that they access (Snider and McMahon, 1998; Woolf and Ma, 2008). These studies have provided an anatomical basis for the functional segregation of nociceptive and non-nociceptive somatosensory neurons. In addition, they have shown that, even among nociceptive neurons, there exists a surprising degree of anatomical and neurochemical specialization, raising the possibility that functional distinctions exist among classes of nociceptors.

Primary afferent neurons

The detection of external somatosensory stimuli is initiated by primary sensory neurons that have their cell bodies in the trigeminal and dorsal root ganglia (DRG), extend a single, bifurcated axon that sends an efferent branch to innervate peripheral target tissues, and a central, afferent branch that targets

regions of the spinal cord dorsal horn or medulla (Woolf and Ma, 2007). Somatosensory primary afferent neurons are traditionally divided based on size, degree of myelination, and conduction velocity into three classes: Aß, Aδ, and C fibers (Erlangen and Gasser, 1924; Julius and Basbaum, 2001). These physiological differences are accompanied by distinct functional contributions of the different neuronal classes to somatosensation. Thus, cell bodies with the largest diameter give rise to myelinated Aß fibers that rapidly conduct nerve impulses and detect innocuous mechanical stimulation. In contrast, noxious thermal and mechanical stimuli are detected by medium diameter, thinly myelinated Aδ fibers and small diameter, unmyelinated, C fibers. These latter classes of primary sensory neurons are therefore known as nociceptors, and represent a dedicated system for the detection of stimuli capable of causing tissue damage (Sherrington, 1906).

Primary afferent nociceptors

Nociceptor subtypes

As noted above, nociceptors are primarily made up of myelinated Aδ fibers and unmyelinated C fibers, which are thought to mediate “first pain” and “second pain”, respectively, based on their speed of transmission (Fields, 1987). The importance of these fiber types for pain responsiveness has been demonstrated by selective nerve block studies (Bishop et al, 1958), and by the fact that a loss of these neurons in humans leads to insensitivity to pain (Indo et al, 1996).

C-fiber nociceptors are subdivided, based on their neurochemical identity, into two broad classes: peptidergic nociceptors, which express the neuropeptides substance P (SP) and calcitonin gene-related peptide (CGRP), and nonpeptidergic nociceptors, which lack neuropeptides and express certain glycoconjugates that bind the lectin IB4 (Snider and McMahon, 1998). In addition, though all unmyelinated fibers show an initial dependence on nerve growth factor (NGF) for survival (Carroll et al, 1992), the nonpeptidergic subset undergoes a switch to glial derived neurotrophic factor (GDNF) sensitivity during development (Molliver et al, 1997). These neuronal groups also show differential expression of several enzymes and receptors. Thus, consistent with their growth factor dependence, peptidergic nociceptors express the NGF receptor trkA, while nonpeptidergic nociceptors contain the GDNF receptor Ret (Molliver et al, 1997). Nonpeptidergic nociceptors also preferentially express the enzyme fluoride-resistant acid phosphatase (FRAP), as well as the ATP-sensitive P2X3 receptor, and several members of the Mrgpr family of G protein-coupled receptors (Snider and McMahon, 1998; Dong et al, 2001). In contrast, at least in the mouse, peptidergic nociceptors contain the predominance of the chemical sensing ion channel, TRPA1 (Story et al, 2003), and the heat and capsaicin receptor, TRPV1 (Zwick et al, 2002). These molecular differences can be attributed in part to different transcription factor regimes at work in peptidergic and nonpeptidergic neurons (Woolf and Ma, 2007).

In addition to these neurochemical differences, peptidergic and nonpeptidergic

nociceptors exhibit a remarkable degree of anatomical segregation. Peptidergic neurons terminate in the outermost laminae of the spinal cord dorsal horn (lamina I and outer lamina II), accessing thalamic and cortical brain areas through lamina I projection neurons, while nonpeptidergic neurons target interneurons in the innermost region of lamina II, which connect to limbic brain areas through lamina V projection neurons (see below for a detailed description of spinal cord circuitry) (Snider and McMahon, 1998; Braz et al, 2005). These populations also have distinct peripheral innervation patterns, with nonpeptidergic axons targeting more superficial cutaneous tissue than their peptidergic counterparts (Zylka et al, 2005).

Electrophysiological recordings

Despite these profound neurochemical and anatomical differences, electrophysiological recordings have identified few functional distinctions between subsets of C-fiber nociceptors. Nociceptors can be characterized based on the sensory modality or modalities (i.e. heat, cold, mechanical, chemical) that are capable of eliciting their activation. Several studies, in species ranging from mice to humans, have demonstrated that, though modality-specific nociceptors exist, the majority are polymodal, in that they are activated by more than one nociceptive modality (Kress et al, 1992; Schmidt et al, 1995; Lawson et al, 2008), and this likely includes both peptidergic and nonpeptidergic phenotypes (Caterina et al, 2000; Lawson et al, 2008). Furthermore, identical percentages of peptidergic and nonpeptidergic nociceptors respond to noxious heat stimuli

(Stucky and Lewin, 1999). It therefore doesn't appear that these nociceptor subtypes can be distinguished based on their general electrophysiological response properties. As a result of this, the prevailing view has been that there is little specificity to the nociceptor, and that it instead acts as a detector of potentially damaging stimuli, regardless of modality (Sherrington, 1906; Perl, 1996).

Nevertheless, some more subtle electrophysiological differences have been identified between nociceptor classes. Thus, peptidergic and nonpeptidergic neurons can be distinguished based on their action potential shape and duration (Stucky and Lewin, 1999; Fang et al, 2006). In addition, nonpeptidergic nociceptors have relatively smaller heat-evoked activation and are generally less excitable than peptidergic nociceptors, leading to the hypothesis that the latter are more relevant for acute heat responses in vivo (Stucky and Lewin, 1999). Furthermore, it has recently been proposed that neurons that stain positive for TRPV1 immunoreactivity, the majority of which are peptidergic, respond selectively to heat (and not mechanical) stimulation, while most IB4-binding neurons have polymodal properties (Lawson et al, 2008). Consistent with this, data from humans has demonstrated that activation of mechanically-sensitive nociceptors with capsaicin, a specific TRPV1 agonist, is much milder than capsaicin-induced activation of mechanically-insensitive neurons (Schmelz et al, 2000).

These results suggest that peptidergic and non-peptidergic nociceptors are not functionally identical, and that the detection of different stimulus modalities may be mediated by a differential contribution from neurochemically-distinct groups of primary afferent neurons. At the same time, at least on a crude level, electrophysiological studies have not shown drastic differences in the relative percentage of neuronal subtypes that are capable of responding to different stimulus modalities. Thus, further studies are necessary to more thoroughly correlate neurochemical identity with electrophysiological properties, and to determine to what extent these nociceptor classes differentially contribute to the pain experience. To that end experimental results reported in this thesis provide some of the first evidence that molecularly-defined nociceptor classes can indeed be segregated based on their contributions to noxious-stimuli-evoked behavior.

Nociceptors and noxious stimulus detection

Acute noxious stimulus detection

The general function of the nociceptive system is to alert the body to stimuli capable of producing tissue injury. The peripheral terminal of the nociceptor is specialized to be able detect such stimuli and transduce them into electrical currents, which propagate down the axon in the form of an action potential (Woolf and Ma, 2007). This process depends on the presence of specific ion channels and receptors at the peripheral terminal, and dozens of these molecules have been identified, including the acid-sensitive ASIC channels, purinergic P2X receptors, voltage-gated sodium, calcium and potassium channels, and the TRP

family of ion channels (Lee et al, 2000; Woolf and Ma, 2007). Notably, many of these molecules are uniquely or preferentially expressed in nociceptors compared to other parts of the nervous system. This includes the sensory neuron specific sodium channels Nav1.8 and 1.9, which contribute to the generation and transduction of action potentials in primary afferent nociceptors (Cummins et al, 2007). Such molecules represent attractive targets for pharmacological interventions designed to reduce pain, since their specificity allows for the treatment of pain with limited risk of side effects.

When an action potential invades the central terminal of a nociceptor, it causes the release of neurotransmitter, which activates spinal cord neurons in the “pain” pathway. Although glutamate is the predominant neurotransmitter in all nociceptors, peptidergic neurons additionally release SP and CGRP following more sustained or intense noxious stimulation (Julius and Basbaum, 2001). Specific receptors for these neurotransmitters, including NMDA and AMPA receptors for glutamate, NK1 receptors for SP, and CGRP receptors, are located in appropriate regions of the spinal cord dorsal horn, and mediate the post-synaptic response to primary afferent activation (Ye et al, 1999; Todd and Koerber, 2006).

Sensitization of nociceptors following tissue injury

Under conditions of tissue injury, the pain system becomes sensitized such that previously innocuous stimuli are perceived as painful (allodynia), and previously

noxious stimuli become more intensely painful (hyperalgesia) (Cervero and Laird, 1996). Two, often complementary, mechanisms underlie the process of sensitization: peripheral sensitization, of the nociceptor itself, and central sensitization, of downstream CNS neurons in the “pain” pathway (Ji et al, 2003).

Tissue injury causes peripheral sensitization via multiple mechanisms. In addition to directly activating sensory receptors on nociceptors, tissue injury results in the release of pro-inflammatory mediators from primary afferent neurons as well as other, non-neuronal cells. Such mediators include ATP, protons, serotonin, lipids, bradykinin and NGF, and they act on receptors in the peripheral terminal of the nociceptor to increase responsiveness to subsequent stimulation. This often occurs via the activation of second messenger signaling cascades, which directly sensitize sensory channels (Julius and Basbaum, 2001). For example, inflammation causes the release of bradykinin and prostaglandin E2, which decrease the threshold for heat activation of TRPV1 via second messengers such as protein kinase C (Ji et al, 2003).

As a result of the increased peripheral activation associated with tissue injury and inflammation, neurons in the dorsal horn of the spinal cord and downstream nociceptive relay centers also undergo long-term changes in their physiological properties, a process known as central sensitization (Ji et al, 2003). This plasticity is characterized by decreased activation thresholds, increased spontaneous activity, and increased receptive field size, and shares many

properties with other forms of long term plasticity observed in the nervous system, such as an important contribution of NMDA receptor activation (Ji et al, 2003).

Spinal cord organization

The spinal cord dorsal horn is classically divided into five parallel laminae, based on cytoarchitectural features of the neurons in each region (Rexed, 1952). These laminae are also distinguished by the types of somatosensory fibers that target them. Thus, neurons in lamina III and IV are innervated by myelinated fibers underlying innocuous touch, and therefore do not process nociceptive information. In contrast, neurons in laminae I, II, and V receive inputs from nociceptive afferents and are therefore important relays in the transmission of pain-related information to the brain (Todd and Koerber, 2006).

Lamina I is targeted by both Aδ nociceptors and peptidergic C fibers. While primarily receiving nociceptive input, lamina I also contains neurons that appear to selectively encode innocuous sensations such as cooling, itch, and sensual touch (Craig, 2003). Lamina I also contains so-called wide dynamic range (WDR) neurons, which receive convergent input from both nociceptive and non-nociceptive fibers, and as such, encode stimulus intensity ranging from the innocuous to the noxious range (Craig, 2003; Almeida et al, 2004; Todd and Koerber, 2006). Though most lamina I neurons are interneurons that connect to other dorsal horn laminae, a small percentage (~10%) are projection neurons

that access pain centers in the brain, primarily through the spinothalamic tract (Bice and Beal, 1997).

Lamina II, also known as the substantia gelatinosa because of its translucent appearance, can be further subdivided into outer (IIo) and inner (IIi) portions, which receive inputs from peptidergic and nonpeptidergic afferents, respectively. In contrast to lamina I, lamina II neurons are nearly all interneurons that project locally. Finally, lamina V contains WDR projection neurons, which receive disynaptic inputs from lamina II interneurons and monosynaptic inputs from Aß and δ fibers, and, like lamina I neurons, project to areas of the thalamus through the spinothalamic tract (Koerber and Todd, 2006).

Spinal cord neurons access ascending circuits that project to various brain regions implicated in pain processing and sensation, including the thalamus, periaqueductal gray, parabrachial region, reticular formation of the medulla, hypothalamus and amygdala (Almeida et al, 2004). From these areas, nociceptive information is transferred to brain regions involved in sensory-discriminatory (somatosensory cortex) and affective-motivational (insula and anterior cingulate cortex) aspects of pain sensation, as well as to areas involved in modulation of the pain experience (rostral ventromedial medulla) (Almeida et al, 2004; Fields, 2004).

References

Almeida TF, Roizenblatt S, Tufik S (2004) Afferent pain pathways: a neuroanatomical review. *Brain Res* 1000:40-56.

BiceTN, Beal JA (1997) Quantitative and neurogenic analysis of the total population and subpopulations of neurons defined by axon projection in the superficial dorsal horn of the rat lumbar spinal cord. *J Comp Neurol* 388:550-64.

Bishop GH, Landau WM, Jones MH (1958) Evidence for a doubles peripheral pathway for pain. *Science* 3326: 712-14.

Braz JM, Nassar MA, Wood JN, Basbaum AI (2005) Parallel "pain" pathways arise from subpopulations of primary afferent nociceptor. *Neuron* 47:787-93.

Carroll SL, Silos-Santiago I, Frese SE, Ruit KG, Milbrandt J, Snider WD (1992) Dorsal root ganglion neurons expressing trk are selectively sensitive to NGF deprivation in utero. *Neuron* 9:779-88.

Caterina MJ, Leffler A, Malmberg AB, Martin WJ, Trafton J, Petersen-Zeitz KR, Koltzenburg M, Basbaum AI, Julius D (2000) Impaired nociception and pain sensation in mice lacking the capsaicin receptor. *Science* 288:306-13.

Cervero F, Laird JM (1996) Mechanisms of touch-evoked pain (allodynia): A new model. *Pain* 68:13-23.

Craig AD (2003) A new view of pain as a homeostatic emotion. *Trends Neurosci* 26:303-7.

Cummins TR, Dib-Hajj SD, Black JA, Waxman SG (2000) Sodium channels and the molecular pathophysiology of pain. *Prog Brain Res* 129:3-19.

Dong X, Han S, Zylka MJ, Simon MI, Anderson DJ (2001) A diverse family of GPCRs expressed in specific subsets of nociceptive sensory neurons. *Cell* 106:619-32.

Erlangen J, Gasser HS (1924) The compound nature of the action potential of nerve as disclosed by the cathode ray oscillograph. *Am J Physiol* 70:624-66.

Fang X, Djouhri L, McMullan S, Berry C, Waxman SG, Okuse K, Lawson SN (2006) Intense isolectin-B4 binding in rat dorsal root ganglion neurons distinguishes C-fiber nociceptors with broad action potentials and high Nav1.9 expression. *J Neurosci* 26:7281-92.

Fields HL (1987) Pain. New York: McGraw-Hill.

Fields H (2004) State-dependent opioid control of pain. *Nat Rev Neurosci* 5:565-75.

Indo Y, Tsuruta M, Hayashida Y, Karim MA, Ohta K, Kawano T, Mitsubuchi H, Tonoki H, Awaya Y, Matsuda I (1996) Mutations in the TRKA/NGF receptor gene in patients with congenital insensitivity to pain with anhidrosis. *Nat Genet* 13:485-8.

Ji R-R, Kohno T, Moore KA, Woolf CJ (2003) Central sensitization and LTP: Do pain and memory share similar mechanisms? *Trends Neurosci* 26:696-705.

Julius D, Basbaum AI (2001) Molecular mechanisms of nociception. *Nature* 413:203-10.

Kress M, Koltzenburg M, Reeh PW, Handwerker HO (1992) Responsiveness and functional attributes of electrically localized terminals of cutaneous C-fibers in vivo and in vitro. *J Neurophysiol* 68:581-95.

Lawson JJ, McIlwrath SL, Woodbury CJ, Davis BM, Koerber HR (2008) TRPV1 unlike TRPV2 is restricted to a subset of mechanically insensitive cutaneous nociceptors responding to heat. *J Pain* 9:298-308.

Lee Y, Lee CH, Oh U (2000) Painful channels in sensory neurons. *Mol Cells* 20:315-24.

Loeser JD, Treede RD (2008) The Kyoto protocol of IASP Basic Pain Terminology. *Pain* 137:473-7.

Lumpkin EA, Caterina MJ (2007) Mechanisms of sensory transduction in the skin. *Nature* 445:858-65.

Molliver DC, Wright DE, Leitner ML, Parsadanian AS, Doster K, Wen D, Yan Q,Snider WD (1997) IB4-binding DRG neurons switch from NGF to GDNF dependence in early postnatal life. *Neuron* 19:849-61.

Perl ER (1996) Cutaneous polymodal receptors: characteristics and plasticity. *Prog Brain Res* 113:21-37.

Perl ER (2007) Ideas about pain, a historical view. *Nat Rev Neurosci* 8:71-80.

Rexed B (1952) The cytoarchitectonic organization of the spinal cord in the cat. *J Comp Neurol* 96:414-95.

Schmelz M, Schmid R, Handwerker HO, Torebjork HE (2000) Encoding of burning pain from capsaicin-treated human skin in two categories of unmyelinated nerve fibers. *Brain* 123:560-71.

Schmidt R, Schmelz M, Torebjörk HE, Handwerker HO (2000) Mechano-insensitive nociceptors encode pain evoked by tonic pressure to human skin. *Neuroscience* 98:793-800.

Schmidt R, Schmelz M, Forster C, Ringkamp M, Torebjörk E, Handwerker H (1995) Novel classes of responsive and unresponsive C nociceptors in human skin. *J Neurosci* 15:333-41.

Sherrington CS (1906) The integrative action of the nervous system. New York: Scribner.

Snider WD, McMahon SB (1998) Tackling pain at the source: New ideas about nociceptors. *Neuron* 20:629-32.

Story GM, Peier AM, Reeve AJ, Eid SR, Mosbacher J, Hricik TR, Earley TJ, Hergarden AC, Andersson DA, Hwang SW, McIntyre P, Jegla T, Bevan S, Patapoutian A (2003) ANKTM1, a TRP-like channel expressed in nociceptive neurons, is activated by cold temperatures. *Cell* 112:819-29.

Stucky CL, Lewin GR (1999) Isolectin B(4)-positive and -negative nociceptors are functionally distinct. *J Neurosci* 19:6497-505.

Todd AJ, Koerber HR (2006) Neuroanatomical substrates of spinal nociception. In: Textbook of Pain, Fifth Edition (McMahon SB, Koltzenburg M, eds), pp 73-90: Elsevier.

Woolf CJ, Ma Q (2007) Nociceptors—Noxious stimulus detectors. *Neuron* 55:353-64.

Ye Z, Wimalawansa SJ, Westlund KN (1999) Receptor for calcitonin gene-related peptide: Localization in the dorsal and ventral spinal cord. *Neuroscience* 92:1389-97.

Zwick M, Davis BM, Woodbury CJ, Burkett JN, Koerber HR, Simpson JF, Albers KM (2002) Glial cell line-derived neurotrophic factor is a survival factor for isolectin B4-positive, but not vanilloid receptor 1-positive, neurons in the mouse. *J Neurosci* 22:4057-65.

Zylka MJ, Rice FL, Anderson DJ (2005) Topographically distinct epidermal nociceptive circuits revealed by axonal tracers targeted to Mrgprd. *Neuron* 45:17-25.

Chapter 2

MrgprD and TRPV1

Mrgpr family of G protein-coupled receptors (GPCRs)

The *Mrgpr* family of GPCRs was first discovered in a subtractive cDNA screen of DRG neurons from wildtype mice and mice lacking the transcription factor neurogenin 1, which is necessary for the generation of trkA-expressing nociceptive neurons (Dong et al, 2001). It was later independently cloned in a screen for GPCRs in rat DRG RNA (Lembo et al, 2002). In mice, the *Mrgpr* family is comprised of six single copy genes (*MrgprD, MrgprE, MrgprF, MrgprG, MrgprH and MAS1*) as well as three larger subfamilies, which each contain multiple members (*MrgprA, MrgprB and MrgprC*). In comparison, humans have only four functional *Mrgpr* genes, known as *MrgprX1-4*, which are most closely related to mouse *MrgprA* genes (Zylka et al, 2003). Notably, many of these genes are specifically expressed in small diameter DRG neurons, primarily of the nonpeptidergic class, suggesting a role for these receptors in nociception (Dong et al, 2001). Furthermore, several of these receptors are expressed in a non-overlapping fashion within nonpeptidergic nociceptors, thus arguing for further anatomical segregation of neurons within this broad class (Dong et al, 2001). To date, endogenous ligands for Mrgpr receptors have not been identified, though several candidate ligands have been proposed, including RF-amide-related

peptides (Han et al, 2002) and peptide products of the proenkephalin A gene, such as bovine adrenal medulla peptide 22 (BAM22) (Lembo et al, 2002).

MrgprD

MrgprD expression in the mouse has been extensively studied by genetically targeting two axonal tracers: placental alkaline phosphatase (PLAP) and farnesylated enhanced green fluorescence protein (fEGFP), to MrgprD$^+$ neurons (Zylka et al, 2005). These studies, in agreement with previous reports (Dong et al 2001) showed that expression of MrgprD is restricted to a subset of IB4-binding, nonpeptidergic nociceptors that contain P2X3 but lack TRPV1. Interestingly, among peripheral targets, MrgprD$^+$ neurons exclusively innervate cutaneous structures, and are absent from visceral organs (Zylka et al, 2005). Furthermore, compared to CGRP$^+$ peptidergic afferents, MrgprD$^+$ neurons innervate more superficial epidermal regions (Zylka et al, 2005).

Electrophysiological analysis of cultured MrgprD$^+$ DRG cells demonstrated that they exhibit characteristics typical of nociceptors, such as long-duration action potentials, TTX-resistant sodium current, and opioid-sensitive calcium currents (Dussor et al, 2008). Furthermore, these neurons are highly sensitive to ATP, consistent with P2X3 expression, but do not respond to capsaicin, consistent with their lack of TRPV1 channels (Dussor et al, 2008). Thus, MrgprD marks a large proportion of nonpeptidergic nociceptors that innervate cutaneous tissue.

However, though it is present in nociceptive neurons, a direct role for MrgprD in nociception has yet to be discovered.

Transient receptor potential (TRP) channels

TRP channels were first discovered in the fly eye, where in 1969, Cosens and Manning found a drosophila mutant that they called *trp* (for transient receptor potential), because it showed a transient instead of sustained response to light (Cosens and Manning, 1969). The *trp* gene was eventually cloned and shown to encode a calcium-permeable cation channel (Montell and Rubin, 1989; Hardie and Minke, 1992). Subsequently, multiple channels with sequence similarity to drosophila *trp* have been identified in a variety of species, and these channels are collectively known as the TRP family of ion channels (Voets et al, 2005). Interestingly, many of these channels have a known function in sensory transduction.

Since the discovery of drosophila TRP, the search for mammalian homologs has resulted in the identification of 28 *trp*-related genes in mice and 27 in humans (Voets et al, 2005). Mammalian TRPs are classified into 7 subfamilies, named for their first identified members: TRPC, TRPV, TRPM, TRPA, TRPP, TRPML and TRPN (Voets et al, 2005). TRP channels share a common architecture and are structurally related to voltage-gated potassium channels. As such, they are made up of four subunits, each with six transmembrane segments and intracellular N- and C-terminal tails (Benham et al, 2002). Transmembrane segments five and

six and the connecting pore loop make up a pore region that is permeable to cations, and, importantly, shows significant calcium permeability (Benham et al, 2002).

TRPV1

In 1997, Caterina and Julius, using an expression-cloning technique, showed that the expression of a cation channel with high sequence similarity to known TRP channels conferred responsiveness to capsaicin, a vanilloid compound that is the pungent ingredient in chili peppers, as well as to noxious heat (>43^{o}C) (Caterina et al, 1997). This channel, now known as TRPV1, is highly expressed in small diameter primary afferent nociceptors (Tominaga et al, 1998), and in the mouse, is thought to be restricted primarily to neurons with a peptidergic phenotype (Zwick et al, 2002). Subsequent to the cloning of TRPV1, several other mammalian TRP channels have been identified that play a known role in thermosensation and nociception, including the warm-activated channels TRPV3 and TRPV4, and the cold-activated channel TRPM8 (Jordt et al, 2003).

In addition to heat and capsaicin, TRPV1 is activated by numerous other exogenous and endogenous ligands, including vanilloid compounds such as resiniferatoxin, spider toxins, alterations in pH, and membrane-derived lipids such as anandamide (Caterina et al, 1997; Caterina and Julius, 2001; Siemens et al, 2006; Dhaka et al, 2009). Furthermore, TRPV1 can be sensitized by

various intracellular signaling molecules, including PKA, PKC, and receptor-activated PLC (Ramsey et al, 2006).

The response profile of TRPV1, along with its expression in nociceptive neurons, suggested that it makes an important contribution to the cellular and behavioral responses to noxious heat. Such a contribution was confirmed by studies in *Trpv1* knockout mice, which showed a drastic reduction in the number of primary afferent neurons that responded to noxious heat, as well as attenuated acute behavioral responses to noxious heat stimuli (Caterina et al, 2000; Davis et al, 2000). Further, *Trpv1* knockout mice exhibited a complete loss of inflammation-induced heat hypersensitivity. Together, these data demonstrate a necessary contribution of TRPV1 to the detection and behavioral response to noxious heat.

In addition to its known role in the detection of noxious heat stimuli, TRPV1 has been proposed to have a more generalized function in the synaptic physiology of multiple brain areas, including the hippocampus and striatum (Maccarrone et al, 2008; Gibson et al, 2008). In accordance with this, several groups have proposed that TRPV1 is expressed in neurons throughout the brain (Caterina, 2003; Steenland et al, 2006). However, there is considerable disagreement as to the extent and localization of this expression, as reports vary widely between papers, even those using similar methods. Data presented in this thesis help to resolve this issue, as we show, using genetically-driven tracers, that TRPV1 expression is largely restricted to primary afferent nociceptors.

References

Benham CD, Davis JB and Randall AD (2002) Vanilloid and TRP channels: a family of lipid-gated cation channels. *Neuropharmacology* 42:873-88.

Caterina MJ, Schumacher MA, Tominaga M, Rosen TA, Levine JD and Julius D (1997) The capsaicin receptor: a heat-activated ion channel in the pain pathway. *Nature* 389:816-24.

Caterina MJ, Leffler A, Malmberg AB, Martin WJ, Trafton J, Petersen-Zeitz KR, Koltzenburg M, Basbaum AI and Julius D (2000) Impaired nociception and pain sensation in mice lacking the capsaicin receptor. *Science* 288:306-13.

Caterina MJ and Julius D (2001) The vanilloid receptor: a molecular gateway to the pain pathway. *Annu Rev Neurosci* 24:487-517.

Caterina MJ (2003) Vanilloid receptors take a TRP beyond the sensory afferent. *Pain* 105:5-9.

Cosens DJ and Manning A (1969) Abnormal electroretinogram from a Drosophila mutant. *Nature* 224:285-7.

Davis JB, Gray J, Gunthorpe MJ, Hatcher JP, Davey PT, Overend P, Harries MH, Latcham J, Clapham C, Atkinson K, Hughes SA, Rance K, Grau E, Harper AJ, Pugh PL, Rogers DC, Bingham S, Randall A and Sheardown SA (2000) Vanilloid receptor-1 is essential for inflammatory thermal hyperalgesia. *Nature* 405:183-7.

Dhaka A, Uzzell V, Dubin AE, Mathur J, Petrus M, Bandell M and Patapoutian A (2009) TRPV1 is activated by both acidic and basic pH. *J Neurosci* 29:153-8.

Dong X, Han S, Zylka MJ, Simon MI and Anderson DJ (2001) A diverse family of GPCRs expressed in specific subsets of nociceptive sensory neurons. *Cell* 106:619-32.

Dussor G, Zylka MJ, Anderson DJ and McCleskey EW (2008) Cutaneous sensory neurons expressing the Mrgprd receptor sense extracellular ATP and are putative nociceptors. *J Neurophysiol* 99:1581-9.

Gibson HE, Edwards JG, Page RS, Van Hook MJ and Kauer JA (2008) TRPV1 channels mediate long-term depression at synapses on hippocampal interneurons. *Neuron* 57:746-59.

Han SK, Dong X, Hwang JI, Zylka MJ, Anderson DJ and Simon MI (2003) Orphan G protein-coupled receptors MrgA1 and MrgC11 are distinctively activated by RF-amide-related peptides through the Galpha q/11 pathway. *Proc Natl Acad Sci USA* 99:14740-5.

Hardie RC and Minke B (1992) The trp gene is essential for a light-activated Ca2+ channel in Drosophila photoreceptors. *Neuron* 8:643-51.

Jordt SE, McKemy DD and Julius D (2003) Lessons from peppers and peppermint: the molecular logic of thermosensation. *Curr Opin Neurobiol* 13:487-92.

Lembo PM, Grazzini E, Groblewski T, O'Donnell D, Roy MO, Zhang J, Hoffert C, Cao J, Schmidt R, Pelletier M, Labarre M, Gosselin M, Fortin Y, Banville

D, Shen SH, Ström P, Payza K, Dray A, Walker P and Ahmad S (2002) Proenkephalin A gene products activate a new family of sensory neuron-specific GPCRs. *Nat Neurosci* 5:201-9.

Maccarrone M, Rossi S, Bari M, De Chiara V, Fezza F, Musella A, Gasperi V, Prosperetti C, Bernardi G, Finazzi-Agrò A, Cravatt BF and Centonze D (2008) Anandamide inhibits metabolism and physiological actions of 2-arachidonoylglycerol in the striatum. *Nat Neurosci* 11:152-9.

Montell C and Rubin GM (1989) Molecular characterization of the Drosophila trp locus: a putative integral membrane protein required for phototransduction. *Neuron* 2:1313-23.

Ramsey IS, Delling M and Clapham DE (2006) An introduction to TRP channels. *Annu Rev Physiol* 68:619-47.

Siemens J, Zhou S, Piskorowski R, Nikai T, Lumpkin EA, Basbaum AI, King D and Julius D (2006) Spider toxins activate the capsaicin receptor to produce inflammatory pain. *Nature* 444:208-12.

Steenland HW, Ko SW, Wu LJ and Zhuo M. Hot receptors in the brain. *Mol Pain* 2:34.

Tominaga M, Caterina MJ, Malmberg AB, Rosen TA, Gilbert H, Skinner K, Raumann BE, Basbaum AI, Julius D (1998) The cloned capsaicin receptor integrates multiple pain-producing stimuli. *Neuron* 21:531-43.

Voets T, Talavera K, Owsianik G and Nilius B (2005) Sensing with TRP channels. *Nat Chem Biol* 1:85-92.

Zwick M, Davis BM, Woodbury CJ, Burkett JN, Koerber HR, Simpson JF and Albers KM (2002) Glial cell line-derived neurotrophic factor is a survival factor for isolectin B4-positive, but not vanilloid receptor 1-positive, neurons in the mouse. *J Neurosci* 22:4057-65.

Zylka MJ, Dong X, Southwell AL and Anderson DJ (2003) Atypical expansion in mice of the sensory neuron-specific Mrg G protein-coupled receptor family. *Proc Natl Acad Sci USA* 100:10043-8.

Zylka MJ, Rice FL and Anderson DJ (2005) Topographically distinct epidermal nociceptive circuits revealed by axonal tracers targeted to Mrgprd. *Neuron* 45:17-25.

Chapter 3

Neuronal and nonneuronal expression of the heat and capsaicin receptor, TRPV1, revealed by genetically-encoded reporter molecules

Daniel J. Cavanaugh[1], Yaron M. Sigal[2,3], Nirao M. Shah[1], David Julius[2,3] and Allan I. Basbaum[1]

Departments of [1]Anatomy, [2]Physiology and [3]Cellular and Molecular

Pharmacology, University of California, San Francisco, San Francisco CA 94158

Abstract

The heat and capsaicin receptor, TRPV1, is required for the normal detection of painful heat stimuli by primary afferent pain fibers (nociceptors), but the extent to which TRPV1 is expressed in supraspinal and non-neuronal tissues is unclear. Here, we have genetically modified the TRPV1 locus to reveal the distribution of TRPV1 cell bodies and processes with excellent specificity and sensitivity. We find that neuronal TRPV1 expression is largely restricted to primary afferent neurons in the dorsal root, nodose, and trigeminal ganglia and in their central and peripheral axonal projections, with minimal expression in the brain. Additionally, we find widespread TRPV1 expression in a subset of arteriolar smooth muscle cells outside of the central nervous system (CNS). This distribution likely contributes to the profound temperature and vascular changes produced by drugs that target TRPV1, in addition to their traditional action on peripheral nerve terminals.

Introduction

TRPV1 is a non-selective cation channel that is activated by noxious heat (>43^{o}C), protons, vanilloid compounds such as capsaicin and resiniferatoxin, and several membrane-derived lipids, including anandamide (Caterina et al, 1997; Caterina and Julius, 2001). Studies of *Trpv1* knockout mice demonstrated a critical contribution of TRPV1 to the cellular and behavioral responses to noxious heat (Caterina et al, 2000; Davis et al, 2000). Although expression of TRPV1 was originally reported to be restricted to primary afferent nociceptors of the dorsal root (DRG), trigeminal (TG) and nodose ganglia (NG) (Szallasi et al, 1995; Caterina et al, 1997; Tominaga et al, 1998), subsequent studies, using a variety of approaches, argued for a much wider distribution, both in neuronal and non-neuronal tissues (reviewed in Caterina, 2003; Steenland et al, 2006). However, there is considerable disagreement as to the extent to which TRPV1 is expressed outside of the nociceptor. For example, resiniferatoxin binding studies have reported results ranging from a lack of binding in the CNS (Szallasi et al, 1995), to limited binding in a few discrete brain regions (Acs et al, 1996), to widespread binding throughout the brain (Roberts et al, 2004).

In part, the lack of consensus reflects the limitations of traditional approaches to determining expression of a molecule, including variable sensitivity and signal to noise, and susceptibility to false positives. Therefore, to obtain a more direct readout of TRPV1 expression patterns, here we generated a line of knock-in

mice in which two highly sensitive enzymatic reporters, placental alkaline phosphatase (PLAP) and nuclear lacZ (nlacZ) (Shah et al, 2004), are expressed under the control of the endogenous TRPV1 promoter. In addition to providing a very sensitive detection method, background levels of PLAP and nlacZ are negligible in the mouse (Shah et al, 2004), which allows for very discrete localization in neuronal and non-neuronal tissues.

Consistent with our early reports (Caterina et al, 1997; Tominaga et al, 1998), we find robust expression of PLAP and nlacZ in primary afferent neurons, predominantly in the peptidergic population of nociceptors, but we could not confirm previous findings of widespread TRPV1 distribution in the CNS. We also demonstrate that TRPV1 is expressed in a subset of arteriolar smooth muscle cells in peripheral tissues, highlighting an important substrate for the actions of heat, protons, and other TRPV1 agonists on vascular tone. These findings have important implications both for the basic understanding of heat effects on neuronal and non-neuronal tissues, as well as for the development of TRPV1 agonists and antagonists for the treatment of pain.

Results

Robust expression of PLAP and nlacZ in primary afferent neurons

We used gene targeting to drive expression of two reporter genes, PLAP and nlacZ (Fig 1a), under the control of the endogenous TRPV1 promoter. We

inserted an internal ribosome entry site (IRES) immediately downstream of the translational TRPV1 stop codon, followed by PLAP, another IRES, and nlacZ, thereby allowing for the transcription and translation of PLAP and nlacZ without disrupting the coding region of the TRPV1 gene. (Fig. 1a). Heterozygous and homozygous mice carrying the reporter construct (hereafter referred to as $TRPV1^{PLAP\text{-}nlacZ}$ mice) were viable and fertile, and responded normally in behavioral tests of heat nociception (data not shown). Furthermore, immunohistochemical analysis of TRPV1 in $TRPV1^{PLAP\text{-}nlacZ}$ mice demonstrated a pattern of TRPV1 expression in DRG neurons (Fig. 3a) indistinguishable from that observed in wild type mice.

Consistent with previous studies that localized TRPV1 using immunohistochemical or in situ hybridization approaches, we found robust expression of nlacZ and PLAP in primary afferent neurons of the DRG and TG (Fig. 1b, c). The negligible background staining associated with nlacZ and PLAP allowed for the unambiguous identification of labeled cells and processes. The nlacZ, visualized with x-gal staining (Fig. 1b), was restricted to the nuclei of presumptive $TRPV1^{+}$ neurons. In contrast, PLAP histochemistry in the DRG labeled both cell bodies (Fig. 1c; arrowheads) and axonal processes (Fig. 1c; arrows).

We also looked for PLAP expression in tissues targeted by axons that originate from sensory neurons of the DRG and TG. We observed very dense PLAP

staining in the most superficial laminae of the spinal cord, a region targeted by small caliber primary afferent neurons. PLAP$^+$ arborizations in deeper laminae of the cord were also readily detected, most noticeably running down the neck of the dorsal horn and terminating in lamina X, surrounding the central canal (Fig. 1d). Furthermore, PLAP prominently labeled axons that extended along the dorsal column white matter, an area of the cord that, like the superficial dorsal horn, contains cell bodies that express the substance P receptor (Abbadie et al, 1999). Importantly, spinal cord PLAP staining was completely eliminated by intrathecal injection of a high dose (10ug) of the TRPV1 agonist capsaicin (Fig. S1), which selectively destroys TRPV1 fibers in the spinal cord. This indicates that the pattern of PLAP staining indeed arose from TRPV1$^+$ nociceptors. Consistent with this conclusion, we did not detect nlacZ$^+$ neurons in the spinal cord.

PLAP staining also showed extensive axonal labeling of peripheral tissues, including glabrous and hairy skin of the hindpaw (Fig. 1e), bladder (Fig. 1f), cornea (Fig. 1g), trachea (Fig. 8i), and dura (Fig. 8j). Compared to previous studies that reported minimal TRPV1 staining under basal conditions (Ji et al, 2002; Elitt et al, 2006), PLAP histochemistry revealed a much higher density of terminal staining in the skin (Fig 2a-d). PLAP staining in sections of glabrous skin of the paw showed that TRPV1 fibers generally stratify parallel to the epidermal/dermal boundary (Fig. 2b arrows), and send regular projections into the innermost epidermal layers (Fig 2a, arrowheads). Occasionally, we observed

axonal endings that extended more superficially, at times contacting the outermost epidermal layer (Fig. 2c,d, arrows).

nlacZ specifically marks capsaicin-responsive, TRPV1$^+$ DRG Neurons

Capsaicin, the pungent ingredient in chili peppers, selectively activates TRPV1 (Caterina et al, 2000). Therefore, to establish the specificity of nlacZ expression for TRPV1 neurons, we investigated the capsaicin-responsiveness of nlacZ$^+$ DRG neurons in culture. DRG neurons were cultured from 6-week old TRPV1$^{PLAP\text{-}nlacZ}$ mice, and capsaicin responses were assessed using live-cell calcium imaging as a functional readout (Fig. 3a-e). After imaging, the cells were fixed and processed for nlacZ histochemistry. Capsaicin elicited calcium responses in 40% of neurons in culture (n = 568). In good agreement, 36% of cultured neurons were nlacZ$^+$. Importantly, we found that >99% of nlacZ$^+$ neurons responded to capsaicin, demonstrating as expected, that nlacZ is only expressed in TRPV1$^+$ DRG neurons. Furthermore, over >90% of capsaicin-responsive neurons were nlacZ$^+$. This compares with studies reporting that only 20% of capsaicin-responsive DRG neurons are TRPV1-immunoreactive (Breese et al, 2005). Taken together these results demonstrate that nlacZ histochemistry not only provides a sensitive and accurate correlate of functional TRPV1 expression, but also that the sensitivity exceeds that of traditional immunohistochemical techniques.

We also compared the expression of nlacZ and TRPV1 in sections of the DRG (Fig. 4a). Consistent with the calcium imaging results, we found that the great majority (95.0±.4%) of $TRPV1^+$ neurons stained positively for nlacZ. This high degree of overlap shows that nlacZ faithfully recapitulates native TRPV1 expression, in vivo as well as in vitro.

nlacZ is concentrated in unmyelinated peptidergic nociceptors in the DRG

Primary afferent neurons are divided into distinct classes based on their size, degree of myelination, and complement of neurotransmitters and receptors (Snider and McMahon, 1998). Immunohistochemical analysis of TRPV1 in the mouse showed that TRPV1 predominates in the so-called peptidergic class of unmyelinated primary afferent nociceptors, which contains the neuropeptides calcitonin gene-related peptide (CGRP) and substance P (SP). In contrast, TRPV1 is largely absent from unmyelinated non-peptidergic nociceptors (Zwick et al, 2002), which can be illustrated by their binding of isolectin B4 (IB4). Electrophysiological analyses, however, suggested that TRPV1 is, in fact, present in the nonpeptidergic class of neurons, but at levels below the detection limit of immunohistochemical analysis (Breese et al, 2005). We therefore sought to determine the subclasses of neurons that express TRPV1 by performing nlacZ histochemistry on DRG sections followed by immunohistochemical analysis for various molecular markers of the different neuronal subtypes.

Corroborating previous reports, we found that TRPV1 is enriched in peptidergic C-fibers. Thus, 64.0±2.3% of nlacZ$^+$ DRG neurons co-labeled for CGRP (Fig. 4b). Furthermore, 82.4±1.3% of SP$^+$ cells and 48.9±1.9% of CGRP$^+$ cells were nlacZ$^+$ (Fig. 4b, c). As SP primarily marks unmyelinated peptidergic nociceptors, while CGRP is expressed in both myelinated and unmyelinated peptidergic afferents, these results suggest that TRPV1$^+$ cells account for the vast majority of the unmyelinated, peptidergic subtype. In contrast, only 11.5±0.7% of nlacZ$^+$ neurons bound IB4 (Fig. 4d). This number is slightly higher than that obtained using antibodies to localize TRPV1 (Zwick et al, 2002), presumably due to the enhanced sensitivity of nlacZ staining compared to TRPV1 immunohistochemistry. However, it is in general agreement with the finding that TRPV1 is largely excluded from this DRG subpopulation. Finally, we found that the vast majority of nlacZ$^+$ neurons are unmyelinated C-fibers, as only a small percentage (3.3±2.1%) expressed the neurofilament N52 (Fig. 4e), which marks neurons with myelinated afferents. Interestingly, given the percentage of nlacZ$^+$ neurons that co-labels with these various markers, it is clear that a fairly large percentage (~20%) of TRPV1$^+$ neurons are negative for both peptidergic and non-peptidergic markers, which indicates that the peptidergic and non-peptidergic classes of C-fiber do not account for the entirety of unmyelinated primary afferent neurons.

It should be noted that, for technical reasons, these percentages were determined following overnight 37^{o}C incubation in the nlacZ reaction solution.

Longer incubations revealed a larger percentage of nlacZ$^+$ neurons, but immunostaining for the various markers was lost or significantly attenuated, making double label studies impossible. For example, when we incubated overnight, we found that 18.4±4.5% of total DRG neurons were nlacZ$^+$, compared to 32.0±2.6% following extended (3 d) incubation (Fig. 4f). Thus, it is possible that these double labeling studies underestimate the overall percentage of any given marker that is nlacZ$^+$, especially for subtypes of neurons that express low levels of TRPV1, which has been suggested for the nonpeptidergic subset.

TRPV1 expression following tissue or nerve injury

Tissue and nerve injury result in alterations of DRG neurochemistry, and these changes can either contribute to or counteract the development of pain hypersensitivity. For example, inflammatory tissue injury, produced by injection of Complete Freund's Adjuvant (CFA), was reported to increase the number of TRPV1$^+$ DRG neurons, thereby contributing to the heat hypersensitivity that follows inflammation (Ji et al, 2002; Breese et al, 2005). Surprisingly, however, we observed no change in the total percentage of nlacZ$^+$ DRG neurons either 2 or 5 days following CFA injection (results not shown). We also saw no change in the density of PLAP staining in the spinal cord or skin in inflamed versus noninflamed tissue (results not shown). Our results thus demonstrate that any inflammation-induced increase in TRPV1 protein must occur in neurons already expressing TRPV1 message.

In contrast to the inflammation-induced upregulation of TRPV1, Michael and Priestley (1999) found that axotomy of DRG neurons downregulates TRPV1 mRNA expression, most likely due to a loss of trophic support from peripheral tissues. In agreement with this, we found that sciatic nerve transection significantly reduced PLAP staining in the spinal cord (Fig. S1c). Importantly, the loss was restricted to the medial aspect of the spinal cord, where sciatic nerve afferents terminate. Thus, as in the rat, nerve injury downregulates TRPV1 transcription in the mouse.

Developmental timecourse of PLAP and nlacZ expression

We investigated the developmental timecourse of nlacZ expression by staining whole embryo sections at different developmental stages. Although previous studies using TRPV1 antibodies first detected expression in DRG at E13.5 (Tamura et al, 2005; Funakoshi et al, 2006), a more recent study demonstrated that a small percentage of cultured embryonic DRG neurons exhibit capsaicin responsiveness at E12.5 (Hjerling-Leffler et al, 2007). Consistent with this latter study, we first detected nlacZ in DRG neurons at E12.5 (Fig. 5b, arrows). At this stage, only a very small percentage of DRG cells were nlacZ+, but the number increased dramatically by E13.5 (Fig 5c), appeared to peak at E14.5 (Fig 5d), and then decreased somewhat by E16.5 (Fig 5e). It thus appears that TRPV1 is expressed in a larger percentage of DRG neurons during development as compared to its final distribution in the adult. Consistent with this, 45.4±4.4% of

DRG neurons were nlacZ$^+$ at P8, and this percentage dropped to adult levels (33.7±1.3%) by P15.

Restricted brain expression of TRPV1

Expression of TRPV1 in the brain has been reported by several groups, using a variety of methods, including pharmacological characterization (Steenland et al, 2006), immunohistochemistry (Liapi and Wood, 2005; Toth et al, 2005; Cristino et al, 2006), in situ hybridization (Mezey et al, 2000), radioligand binding (Acs et al, 1996; Roberts et al, 2004), Northern blot (Sanchez et al, 2001) and RT-PCR (Sasamura et al, 1998; Mezey et al, 2000). Despite the abundance of studies, the existence of TRPV1 in the brain remains a controversial topic, largely because the extent and localization of TRPV1 varies considerably among studies, even those using very similar assays.

Importantly, we found no evidence of PLAP$^+$ cell bodies in the brain or spinal cord. Indeed, most PLAP staining in the brain of TRPV1$^{PLAP\text{-}nlacZ}$ mice was restricted to areas that receive direct projections from primary afferent neurons. For example, we observed dense PLAP axonal staining in the superficial layers of the nucleus caudalis (Fig. 4a, arrow), which is targeted by TG afferents, as well as in the nucleus of the solitary tract (NTS; Fig. 4a, arrowhead) and in the area postrema of the medulla, both of which are innervated by vagal afferents originating in the nodose ganglion. Consistent with expression in the NTS, we noted robust PLAP staining of the solitary tract (Fig. 4b, arrow). We also found

nlacZ expression in the nodose ganglion (Figure S2). Interestingly, the overlap of IB4 binding with nlacZ in the nodose ganglion was significantly greater than in the DRG; (38.2±3.2% of nodose nlacZ$^+$ cells were IB4$^+$).

The great sensitivity of the PLAP detection method is further illustrated by our observation of extended trigeminal afferent terminal fields in the brainstem. For example, we found PLAP expression in axons extending from the ventromedial border of nucleus caudalis into the region of the rostral ventrolateral reticular nucleus, raising the possibility of a monosynaptic input from TRPV1 positive afferents to motor neurons of the nucleus ambiguous (Fig. 6c). Strikingly, we also observed PLAP$^+$ axons projecting throughout the parabrachial nucleus (Fig. 6e, f, arrows), with especially dense terminations in the CGRP$^+$ cell body rich, external lateral parabrachial nucleus (Fig. 6e, arrow; Fig. S3). Finally, we found extensive axonal PLAP staining in the granule layer of the olfactory bulb (Fig. 6d), as well as sparser innervation of the glomerular region of the bulb. Importantly, PLAP label in the brain, including in the parabrachial nucleus and olfactory bulb, was completely eliminated following systemic administration of the neurotoxic TRPV1 agonist, resiniferatoxin (RTX) (Fig 9a-c).

Despite these widely distributed PLAP$^+$ fibers in the CNS, we never found PLAP$^+$ cell bodies in the brain. Somewhat paradoxically, however, we did find limited nlacZ expression in several brain areas. We saw light staining in the periaqueductal gray (PAG) (Fig. 7a) and interpeduncular nucleus (Fig. 7b), and

more intense staining in the arcuate nucleus of the hypothalamus Fig. 7c) and the accessory olfactory bulb (Fig. 7d). Finally, we detected nlacZ in a discrete subset of hippocampal neurons (Fig. 7e) that co-labeled for reelin (Fig. 7f), a marker of Cajal-Retzius cells. It is unclear why we failed to observe PLAP in these brain regions, but it is likely that the greater sensitivity of nlacZ versus PLAP histochemistry accounts for this discrepancy. However, we cannot rule out the possibility that nlacZ staining in the brain resulted from spurious transcription of nlacZ, in the absence of TRPV1. Consistent with this possibility, the nlacZ staining in the brain was unaltered either by systemic RTX (data not shown), or by direct microinjection of RTX into the hippocampus.

Evidence for TRPV1 in arteriolar smooth muscle cells

Unexpectedly, when examining peripheral tissue for the presence of PLAP-containing axons, we noticed discrete, train track-like staining, often running perpendicular to blood vessels (Fig. 8b, h-j; arrows). This pattern of staining was easily distinguished from the thin, tortuous label associated with axonal PLAP. Importantly, we found comparable patterns of nlacZ staining in the periphery (Fig. 8a, c-g; arrows), demonstrating that the PLAP derived from TRPV1$^+$ cells that are intrinsic to these tissues. Double label for nlacZ and with an antibody directed against alpha smooth muscle actin (SMA), a filament that is specifically associated with smooth muscle cells, revealed that the TRPV1 reporters indeed colocalized with SMA (Fig. 8f).

Interestingly, the PLAP and nlacZ expression was limited to a small, but consistent, subset of vessel smooth muscle cells. For example, we detected expression in various tissues, including the cremaster muscle (Fig. 8a, b), tongue (Fig. 8c, d), TG (Fig. 8e), fat (Fig. 8f), skin (Fig. 8g, h), trachea (Fig 8i), and dura (Fig 8j). Smooth muscle label was largely absent in other organs, including the liver, lung, kidney, pancreas, spinal cord, brain, and the ascending aorta. Further, even within tissue where we saw extensive smooth muscle staining, expression was restricted to certain small to medium diameter vessels (>70 μm in diameter) Thus, as in Fig. 6b, d and j, there were clearly unlabeled vessels (arrowheads) in close apposition to labeled vessels (arrows). Given their size and location, the labeled blood vessels are most likely arterioles. Importantly, using RT-PCR for TRPV1 mRNA, we confirmed that the vascular PLAP and nlacZ labeling indeed represented local translation of TRPV1 mRNA (Fig. 7g). Furthermore, the smooth muscle label was substantially reduced following systemic resiniferatoxin, thus demonstrating that TRPV1 expression is functional in these tissues (Fig. 9d and e).

Discussion

Although a critical role for TRPV1 in heat transduction and nociception has been known for some time, it remains unclear how widespread is the expression of this molecule. Many groups, using a variety of techniques (almost exclusively in the rat), have reported that TRPV1 is present throughout the brain, as well as in

other, non-neuronal tissues (Acs et al, 1996; Sasamura et al, 1998; Mezey et al, 2000; Sanchez et al, 2001; Roberts et al, 2004; Liapi and Wood, 2005; Toth et al, 2005; Cristino et al, 2006). There is, however, considerable disagreement as to the extent and localization of this expression, as reports vary widely between papers, even those using similar methods. To help resolve this issue, we generated mice that express two reporter molecules, PLAP and nlacZ, under the control of the endogenous TRPV1 promoter.

In agreement with the known function of TRPV1 in primary afferent neurons, we found robust expression of both PLAP and nlacZ in the DRG, TG and NG. The fidelity and sensitivity of these reporter molecules were confirmed by calcium imaging experiments, thereby establishing the utility of the TRPV1$^{PLAP\text{-}nlacZ}$ mouse as a tool to accurately determine TRPV1 expression. Importantly, the excellent sensitivity of PLAP staining allowed for a much greater appreciation of the extent of primary afferent innervation of both central and peripheral tissues than was previously reported using traditional immunohistochemical techniques. The greater signal to noise ratio and minimal background using PLAP and nlacZ is particularly advantageous compared to studies using TRPV1 antisera. For example, while others reported barely detectable levels of TRPV1 protein in the skin under basal conditions (Ji et al, 2002; Breese et al, 2005; Elitt et al, 2006), we observed dense axonal arbors coursing throughout the skin. We also observed a much denser corneal innervation than did an immunohistochemical analysis (Murata and Masuko, 2006), and we found extensive PLAP labeling in

the olfactory bulb. Although this area is known to be innervated by peptidergic trigeminal fibers (Finger and Bottger, 1993), the extent of innervation that we see has not previously been appreciated, especially with regard to the granule layer of the bulb. Finally, we observed clear PLAP labeling in axons throughout the parabrachial nucleus, which suggests that this region receives significant direct primary afferent input. Notably, the densest PLAP staining in the parabrachial nucleus was in the external lateral portion, which is known to receive indirect nociceptive input via the spinoparabrachial pathway (Feil and Herbert, 1995). Direct access of primary afferent neurons to the parabrachial nucleus would provide an alternative circuit that could contribute, in addition to the spinoparabrachial pathway, to nociceptive modulation of parabrachial output. That this PLAP staining derives from primary afferents, and not from the nlacZ^{+} cells in the brain, is strongly supported by the fact that systemic resiniferatoxin eliminates PLAP staining without affecting nlacZ expression in the CNS.

The remarkable sensitivity of our approach is also demonstrated by the fact that we observed prominent PLAP and nlacZ expression in arteriolar smooth muscle cells, where TRPV1 expression, as determined by more traditional techniques, has not always been appreciated. Nevertheless, it has long been hypothesized that capsaicin has direct effects on smooth muscle cells, in addition to its indirect effects via activation of vessel-associated nerves (Duckles, 1986). Recently, a group showed the presence of TRPV1 on rat smooth muscle cells using immunohistochemistry and RT-PCR (Kark et al, 2008). They additionally

demonstrated a non-neurogenic constriction by capsaicin of blood vessels in striated muscle. We further these observations by showing evidence that, as in the rat, TRPV1 is expressed in smooth muscle cells of the mouse. Interestingly, we noted the selective expression of PLAP and nlacZ on a subset of arteriolar smooth muscle cells of certain peripheral tissues. TRPV1 mRNA expression in these tissues was confirmed by RT-PCR experiments, and functional TRPV1 protein was demonstrated by the fact that smooth muscle cell label was substantially reduced following systemic resiniferatoxin injection. Notably, many of the areas that we observed $TRPV1^{+}$ smooth muscle cells (tongue, skin, trachea, cremaster, fat tissue) are thermoregulatory in nature. Thus, arteriolar TRPV1 is ideally localized to mediate the effects of temperature and pH on vascular tone.

Recently, a number of studies using *Trpv1* knockout mice have argued for the existence of TRPV1 in supraspinal and non-neuronal tissues, including urothelial cells of the bladder (Birder et al, 2002), osmosensitive neurons of the supraoptic and paraventricular regions of the hypothalamus (Ciura and Bourque, 2006; Sharif Naeini et al, 2006; Sharif-Naeini et al, 2008), taste cells of the tongue (Lyall et al, 2004), as well as neurons in the striatum (Maccarrone et al, 2008) and hippocampus (Marsch et al, 2007; Gibson et al, 2008). Surprisingly, analysis of $TRPV1^{PLAP\text{-}nlacZ}$ mouse tissue failed to corroborate any of these studies. We did not detect evidence for $TRPV1^{+}$ cell bodies in any of the regions indicated by the knockout studies, either by PLAP or nlacZ histochemistry, or by RT-PCR.

Although we did see nlacZ cells in the hippocampus, double labeling with reelin demonstrated that nlacZ labels a subset of hippocampal neurons known as Cajal-Retzius cells, while knockout studies implicate pyramidal cells in regions CA1 and CA3 of the hippocampus. Consistent with the absence of PLAP and nlacZ observed in this study, others have reported a lack of evidence for functional TRPV1 in several candidate regions, including bladder urothelial cells (Yamada et al, 2008), hypothalamus (Taylor et al, 2008), and hippocampus (Kofalvi et al, 2006). Thus, despite the identification of physiological differences between *Trpv1* knockout and wildtype mice in knockout studies, we would caution that additional anatomical analysis is needed to unequivocally demonstrate that TRPV1 in the brain is contributing to these differences, especially as many of these studies fail to show anatomical evidence of TRPV1 in the brain regions of interest.

$TRPV1^{PLAP\text{-}nlacZ}$ mice therefore offer a sensitive and accurate means for studying TRPV1 expression in the mouse. This tool helps to resolve an important issue regarding the extent of TRPV1 expression outside the primary afferent nociceptor, and therefore furthers our basic understanding of temperature and pH effects on neuronal and non-neuronal tissues. Finally, it provides important insight into potential side effects associated with the TRPV1 agonists and antagonists that are currently being developed for the treatment of pain conditions.

Materials and Methods

Generation of TRPV1$^{PLAP\text{-}nlacZ}$ Mice

A 129Sv BAC clone (Geneservice, Ltd.) spanning the 3' end of the TRPV1 gene was used to generate the targeting vector for embryonic stem (ES) cell electroporation. A 6.2kb genomic region containing 2.5kb upstream and 3.7kb downstream of the TRPV1 stop codon was isolated by restriction digest and cloned into the pBluescript II vector. Site-directed mutagenesis was used to engineer an AscI site 3bp downstream of the TRPV1 stop codon of this 6.2kb genomic fragment. A cassette containing IRES-PLAP-IRES-nlacZ and a self-excising *loxP*-flanked, neomycin-resistant cassette (ACN) (Bunting et al., 1999; Shah et al., 2004) was then inserted into this targeting vector as a 12.5kb AscI fragment.

The resulting targeting vector was electroporated into E14 ES cells followed by G418 selection. Surviving ES clones were screened for correct targeting by Southern Blot and PCR and correctly targeted clones were sent for blastocyst injection. Resulting male chimeric mice were bred to C57B/6 females and germline transmission resulted in offspring heterozygous for the mutant allele. Since the ACN construct contains a self-excising neo cassette, heterozygous offspring of chimeras lack this portion of the reporter construct (Bunting et al, 1999).

PLAP and nlacZ Detection

PLAP: Adult mice were perfused with 10mL hepes-buffered saline (HBS) followed by 20mL of ice cold 3.7% formaldehyde. Brain, spinal cord, peripheral tissue, DRG, TG and NG were dissected out, post-fixed 3-4 hours at 4^{o}C and cryoprotected overnight (ON) in 30% sucrose. For brain and spinal cord, 40-80μm microtome sections were cut and tissue was processed as free-floating sections. For DRG, TG, NG, tongue, and skin, 14μm cryostat sections were cut and tissue was processed on slides. Peripheral tissues (skin, cornea, bladder, cremaster, TG, trachea) were processed as whole mounts.

Sections were collected in ice-cold HBS and then rinsed several times with room temperature HBS. Endogenous alkaline phosphatase activity was inactivated by a 60-90 minute incubation in 72^{o}C HBS. Following heat-inactivation, sections were rinsed in room temperature HBS, washed 3 x 5 minutes in B1 buffer (.1M Tris, pH7.5; .15M NaCl) and 3 x 5 minutes in B3 buffer (.1M Tris, pH9.5; .1M NaCl; 50mM $MgCl_2$). PLAP was visualized by incubating sections ON in .2mg/mL BCIP (Roche) and 1mg/mL NBT (Roche) in B3 buffer. The reaction was stopped by washing several times in HBS containing 1mM EDTA.

Sections were then fixed for at least one hour in 3.7% formaldehyde at 4^{o}C and destained with a series of dehydration and rehydration steps in ethanol until desired signal to noise was reached. Sections were rinsed in HBS and then mounted with Fluoromount G (Southern Biotech).

nlacZ: Tissue for nlacZ detection was processed as described above except post-fixation time was limited to 1-1.5 hours to preserve enzyme activity. Sections were rinsed in Solution A (phosphate buffered saline (PBS) with 2mM $MgCl_2$), rinsed briefly with pre-warmed (37^oC) Solution B (.1M NaPO4; 2mM $MgCl_2$; .2% NP40; .1% Na deoxycholate) and then incubated 1-3 d in Solution C (Solution B + .5M K ferrocyanide; .5M K ferricyanide; .6mg/mL X-Gal) at 37^oC.

The reaction was stopped with HBS containing 1mM EDTA. Sections were then fixed for at least one hour in 3.7% formaldehyde at 4^oC, rinsed with HBS and mounted with Fluoromount G.

Immunohistochemistry

Following PLAP or nlacZ histochemistry, tissue was processed for immunohistochemistry as previously described (Shields et al, 2007). Primary antisera were as follows: guinea pig anti-TRPV1 (1:1000; gift of D. Julius, UCSF), rabbit anti-βgal (1:10000; Cappel), rabbit anti-CGRP (1:1000; Peninsula), guinea pig anti-SP (1:8000; gift of J. Maggio, University of Cincinnati), mouse anti-N52 (1:1000; Sigma), mouse anti-reelin (1:500; Chemicon), mouse anti-SMA, (1:800; Sigma). For IB4 binding, we added biotinylated IB4 (1:500; Vector Laboratories) instead of primary antiserum. For double labeling images with x-gal staining followed by immunohistochemistry, x-gal reaction product was pseudocolored magenta so that these images could be overlayed with fluorescent immunohistochemical images. For cell counting, 5 sections of L4/5 DRG or

nodose ganglion were counted for each of three animals, and percentages are given as mean ± standard error measure.

RT-PCR

Adult mice were perfused with 10 mL PBS followed by 10 mL RNA later (Ambion). TG, liver, bladder, and cremaster were dissected out and placed in RNA later on ice. For brain regions, 500 μm brain sections were cut with a McIlwain Tissue Chopper into ice cold PBS, and brain regions were microdissected out with sharp tissue forceps and put into RNA later on ice. To avoid contamination, separate forceps were used for dissection of each tissue/brain region.

RNA isolation was performed with TRIzol reagent (Sigma) according to the manufacturers specifications. 1 μg of each RNA was reverse transcribed with SuperScript II Reverse Strand Synthesis System (Invitrogen) using an oligo (dT) primer. Control reactions omitted reverse transcriptase. PCR amplification (94°C for 5 min; 35 cycles of 94°C for 30 s, 58°C for 30 s, 72°C for 1 min; 72°C for 10 min) was performed with 1 μl of cDNA using the following primer pair: 5'-gtttgtggacagctacagtg-3' and 5'-gaagccacatactccttgcg-3'. Then, to increase sensitivity, 2 μl of this PCR reaction was submitted to another 35 cycle PCR using the same cycling parameters and primers. Control PCR amplification (94°C for 5 min; 25 cycles of 94°C for 30 s, 58°C for 30 s, 72°C for 1 min; 72°C for 10 min) was performed with a GAPDH primer pair (5'-accacagtccatgccatcac-3' and

5’-tccaccaccctgttgctgta-3’) to ensure cDNA integrity. Amplification products were visualized on a 1% agarose gel with ethidium bromide and sequenced to confirm identity.

Calcium Imaging

DRG neurons were isolated from 6 week old mice and dissociated with 0.125% collagenase P (Boehringer) solution in CMF Hank's solution at 37°C for 20 min, pelleted, and resuspended in 0.25% trypsin at 37°C for 2 min. Ganglia were triturated gently with a fire-polished Pasteur pipette in culture medium (MEM Eagle's/Earle's BSS with 10% fetal bovine serum, vitamins, penicillin–streptomycin, l-glutamine), cultured overnight on poly-D-lysine coated coverslips, and subjected to ratiometric calcium imaging the next day. Cells were loaded with 10 μm Fura-2-AM (Molecular Probes) at 22–25 °C for 60 min in extracellular Ringer's solution (140 mM NaCl, 5 mM KCl, 2 mM CaCl2, 1 mM MgCl2, 10 mM D-glucose and 10 mM sodium HEPES, pH 7.4). Cells were illuminated using a xenon light source and filter wheel (Lambda LS and Lambda-10, Sutter Instruments) for 300 ms, alternately at 350 nm and 380 nm (band-pass filters from Chroma Technology). Fluorescence emission at >480 nm (long-pass filter from Chroma Technology) was captured with an intensified CCD camera (Hamamatsu) and was digitized, background corrected and analyzed with the MetaFluor imaging system (Molecular Devices). Background-corrected 340/380 ratio images were collected every 3 s. Cells were stimulated with 1 μM capsaicin, followed by High K+ Ringer’s Solution, then fixed and stained for x-gal

histochemistry. All neurons that responded to HiK+ solution were included for analysis.

References

Abbadie C, Skinner K, Mitrovic I, Basbaum AI (1999) Neurons in the dorsal column white matter of the spinal cord: complex neuropil in an unexpected location. *Proc Natl Acad Sci U S A* 96:260-265.

Acs G, Palkovits M, Blumberg PM (1996) Specific binding of [3H]resiniferatoxin by human and rat preoptic area, locus ceruleus, medial hypothalamus, reticular formation and ventral thalamus membrane preparations. *Life Sci* 59:1899-1908.

Birder LA, Nakamura Y, Kiss S, Nealen ML, Barrick S, Kanai AJ, Wang E, Ruiz G, De Groat WC, Apodaca G, Watkins S, Caterina MJ (2002) Altered urinary bladder function in mice lacking the vanilloid receptor TRPV1. *Nat Neurosci* 5:856-860.

Breese NM, George AC, Pauers LE, Stucky CL (2005) Peripheral inflammation selectively increases TRPV1 function in IB4-positive sensory neurons from adult mouse. *Pain* 115:37-49.

Bunting M, Bernstein KE, Greer JM, Capecchi MR, Thomas KR (1999) Targeting genes for self-excision in the germ line. *Genes Dev* 13:1524-1528.

Caterina MJ (2003) Vanilloid receptors take a TRP beyond the sensory afferent. *Pain* 105:5-9.

Caterina MJ, Julius D (2001) The vanilloid receptor: a molecular gateway to the pain pathway. *Annu Rev Neurosci* 24:487-517.

Caterina MJ, Schumacher MA, Tominaga M, Rosen TA, Levine JD, Julius D (1997) The capsaicin receptor: a heat-activated ion channel in the pain pathway. *Nature* 389:816-824.

Caterina MJ, Leffler A, Malmberg AB, Martin WJ, Trafton J, Petersen-Zeitz KR, Koltzenburg M, Basbaum AI, Julius D (2000) Impaired nociception and pain sensation in mice lacking the capsaicin receptor. *Science* 288:306-313.

Ciura S, Bourque CW (2006) Transient receptor potential vanilloid 1 is required for intrinsic osmoreception in organum vasculosum lamina terminalis neurons and for normal thirst responses to systemic hyperosmolality. *J Neurosci* 26:9069-9075.

Cristino L, de Petrocellis L, Pryce G, Baker D, Guglielmotti V, Di Marzo V (2006) Immunohistochemical localization of cannabinoid type 1 and vanilloid transient receptor potential vanilloid type 1 receptors in the mouse brain. *Neuroscience* 139:1405-1415.

Davis JB, Gray J, Gunthorpe MJ, Hatcher JP, Davey PT, Overend P, Harries MH, Latcham J, Clapham C, Atkinson K, Hughes SA, Rance K, Grau E, Harper AJ, Pugh PL, Rogers DC, Bingham S, Randall A, Sheardown SA (2000) Vanilloid receptor-1 is essential for inflammatory thermal hyperalgesia. *Nature* 405:183-187.

Duckles SP (1986) Effects of capsaicin on vascular smooth muscle. *Naunyn Schmiedebergs Arch Pharmacol* 333:59-64.

Elitt CM, McIlwrath SL, Lawson JJ, Malin SA, Molliver DC, Cornuet PK, Koerber HR, Davis BM, Albers KM (2006) Artemin overexpression in skin enhances expression of TRPV1 and TRPA1 in cutaneous sensory neurons and leads to behavioral sensitivity to heat and cold. *J Neurosci* 26:8578-8587.

Feil K, Herbert H (1995) Topographic organization of spinal and trigeminal somatosensory pathways to the rat parabrachial and Kolliker-Fuse nuclei. *J Comp Neurol* 353:506-528.

Finger TE, Bottger B (1993) Peripheral peptidergic fibers of the trigeminal nerve in the olfactory bulb of the rat. *J Comp Neurol* 334:117-124.

Funakoshi K, Nakano M, Atobe Y, Goris RC, Kadota T, Yazama F (2006) Differential development of TRPV1-expressing sensory nerves in peripheral organs. *Cell Tissue Res* 323:27-41.

Gibson HE, Edwards JG, Page RS, Van Hook MJ, Kauer JA (2008) TRPV1 channels mediate long-term depression at synapses on hippocampal interneurons. *Neuron* 57:746-759.

Hjerling-Leffler J, Alqatari M, Ernfors P, Koltzenburg M (2007) Emergence of functional sensory subtypes as defined by transient receptor potential channel expression. *J Neurosci* 27:2435-2443.

Ji RR, Samad TA, Jin SX, Schmoll R, Woolf CJ (2002) p38 MAPK activation by NGF in primary sensory neurons after inflammation increases TRPV1 levels and maintains heat hyperalgesia. *Neuron* 36:57-68.

Kark T, Bagi Z, Lizanecz E, Pasztor ET, Erdei N, Czikora A, Papp Z, Edes I, Porszasz R, Toth A (2008) Tissue-specific regulation of microvascular diameter: opposite functional roles of neuronal and smooth muscle located vanilloid receptor-1. *Mol Pharmacol* 73:1405-1412.

Kofalvi A, Oliveira CR, Cunha RA (2006) Lack of evidence for functional TRPV1 vanilloid receptors in rat hippocampal nerve terminals. *Neurosci Lett* 403:151-156.

Liapi A, Wood JN (2005) Extensive co-localization and heteromultimer formation of the vanilloid receptor-like protein TRPV2 and the capsaicin receptor TRPV1 in the adult rat cerebral cortex. *Eur J Neurosci* 22:825-834.

Lyall V, Heck GL, Vinnikova AK, Ghosh S, Phan TH, Alam RI, Russell OF, Malik SA, Bigbee JW, DeSimone JA (2004) The mammalian amiloride-insensitive non-specific salt taste receptor is a vanilloid receptor-1 variant. *J Physiol* 558:147-159.

Maccarrone M, Rossi S, Bari M, De Chiara V, Fezza F, Musella A, Gasperi V, Prosperetti C, Bernardi G, Finazzi-Agro A, Cravatt BF, Centonze D (2008) Anandamide inhibits metabolism and physiological actions of 2-arachidonoylglycerol in the striatum. *Nat Neurosci* 11:152-159.

Marsch R, Foeller E, Rammes G, Bunck M, Kossl M, Holsboer F, Zieglgansberger W, Landgraf R, Lutz B, Wotjak CT (2007) Reduced anxiety, conditioned fear, and hippocampal long-term potentiation in transient receptor potential vanilloid type 1 receptor-deficient mice. *J Neurosci* 27:832-839.

Mezey E, Toth ZE, Cortright DN, Arzubi MK, Krause JE, Elde R, Guo A, Blumberg PM, Szallasi A (2000) Distribution of mRNA for vanilloid receptor subtype 1 (VR1), and VR1-like immunoreactivity, in the central nervous system of the rat and human. *Proc Natl Acad Sci U S A* 97:3655-3660.

Murata Y, Masuko S (2006) Peripheral and central distribution of TRPV1, substance P and CGRP of rat corneal neurons. *Brain Res* 1085:87-94.

Roberts JC, Davis JB, Benham CD (2004) [3H]Resiniferatoxin autoradiography in the CNS of wild-type and TRPV1 null mice defines TRPV1 (VR-1) protein distribution. *Brain Res* 995:176-183.

Sanchez JF, Krause JE, Cortright DN (2001) The distribution and regulation of vanilloid receptor VR1 and VR1 5' splice variant RNA expression in rat. *Neuroscience* 107:373-381.

Sasamura T, Sasaki M, Tohda C, Kuraishi Y (1998) Existence of capsaicin-sensitive glutamatergic terminals in rat hypothalamus. *Neuroreport* 9:2045-2048.

Shah NM, Pisapia DJ, Maniatis S, Mendelsohn MM, Nemes A, Axel R (2004) Visualizing sexual dimorphism in the brain. *Neuron* 43:313-319.

Sharif Naeini R, Witty MF, Seguela P, Bourque CW (2006) An N-terminal variant of Trpv1 channel is required for osmosensory transduction. *Nat Neurosci* 9:93-98.

Sharif-Naeini R, Ciura S, Bourque CW (2008) TRPV1 gene required for thermosensory transduction and anticipatory secretion from vasopressin neurons during hyperthermia. *Neuron* 58:179-185.

Shields SD, Mazario J, Skinner K, Basbaum AI (2007) Anatomical and functional analysis of aquaporin 1, a water channel in primary afferent neurons. *Pain* 131:8-20.

Snider WD, McMahon SB (1998) Tackling pain at the source: new ideas about nociceptors. *Neuron* 20:629-632.

Steenland HW, Ko SW, Wu LJ, Zhuo M (2006) Hot receptors in the brain. *Mol Pain* 2:34.

Szallasi A, Nilsson S, Farkas-Szallasi T, Blumberg PM, Hokfelt T, Lundberg JM (1995) Vanilloid (capsaicin) receptors in the rat: distribution in the brain, regional differences in the spinal cord, axonal transport to the periphery, and depletion by systemic vanilloid treatment. *Brain Res* 703:175-183.

Tamura S, Morikawa Y, Senba E (2005) TRPV2, a capsaicin receptor homologue, is expressed predominantly in the neurotrophin-3-dependent subpopulation of primary sensory neurons. *Neuroscience* 130:223-228.

Taylor AC, McCarthy JJ, Stocker SD (2008) Mice lacking the transient receptor vanilloid potential 1 channel display normal thirst responses and central Fos activation to hypernatremia. *Am J Physiol Regul Integr Comp Physiol* 294:R1285-1293.

Tominaga M, Caterina MJ, Malmberg AB, Rosen TA, Gilbert H, Skinner K, Raumann BE, Basbaum AI, Julius D (1998) The cloned capsaicin receptor integrates multiple pain-producing stimuli. *Neuron* 21:531-543.

Toth A, Boczan J, Kedei N, Lizanecz E, Bagi Z, Papp Z, Edes I, Csiba L, Blumberg PM (2005) Expression and distribution of vanilloid receptor 1 (TRPV1) in the adult rat brain. *Brain Res Mol Brain Res* 135:162-168.

Yamada T, Ugawa S, Ueda T, Ishida Y, Kajita K, Shimada S (2008) Differential Localizations of the Transient Receptor Potential Channels TRPV4 and TRPV1 in the Mouse Urinary Bladder. *J Histochem Cytochem* 57: 277-87.

Zwick M, Davis BM, Woodbury CJ, Burkett JN, Koerber HR, Simpson JF, Albers KM (2002) Glial cell line-derived neurotrophic factor is a survival factor for isolectin B4-positive, but not vanilloid receptor 1-positive, neurons in the mouse. *J Neurosci* 22:4057-4065.

Figure 1. PLAP and nlacZ expression in DRG neurons of TRPV1$^{PLAP\text{-}nlacZ}$ mice.

(A) Schematic showing the TRPV1 locus of TRPV1$^{PLAP\text{-}nlacZ}$ mice. A cassette containing IRES-PLAP-IRES-nlacZ has been inserted just downstream of the translational stop codon of the *Trpv1* gene.

(B) nlacZ, visualized with x-gal reaction, is present in nuclei of DRG neurons.

(C) PLAP, visualized with NBT/BCIP staining, is present both in cell bodies (arrowheads) and axonal processes (arrows) of DRG neurons.

(D) PLAP staining in spinal cord dorsal horn.

(E-G) Peripheral PLAP^{+} axons in (E) paw skin (dotted line represents border between glabrous and hairy skin), (F) bladder, and (G) cornea.

Scale bars in B and C = 100μm, in D-G = 200μm.

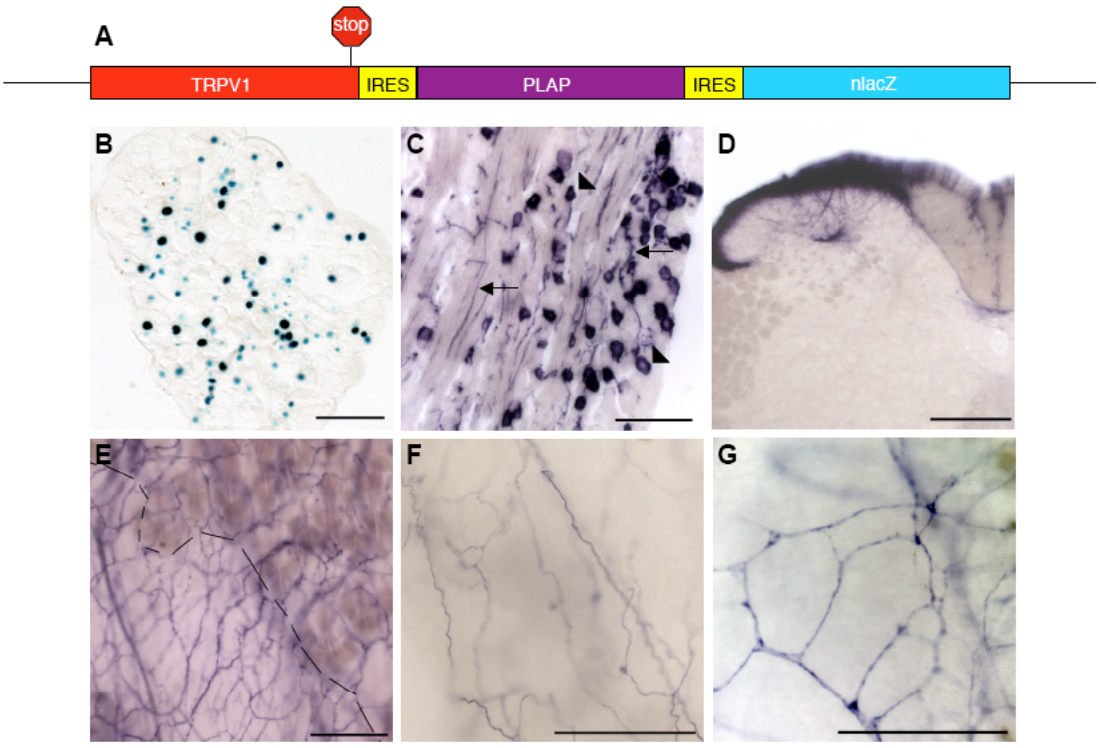
A
stop
TRPV1
IRES
PLAP
IRES
nlacZ
B
C
D
E
F
G

Figure 2. PLAP staining in sections of glabrous paw skin.

(A-D) PLAP staining in 14 μm sections of paw skin.

(A) and (B) $PLAP^+$ afferent fibers were observed running parallel to the dermal/epidermal border (arrows) and regularly extended into the innermost epidermal layers.

(C) and (D) We occasionally observed $PLAP^+$ fibers extending throughout the epidermis. Arrows show axons reaching the outermost layer of the epidermis (stratum granulosum). Scale bars = 200μm.

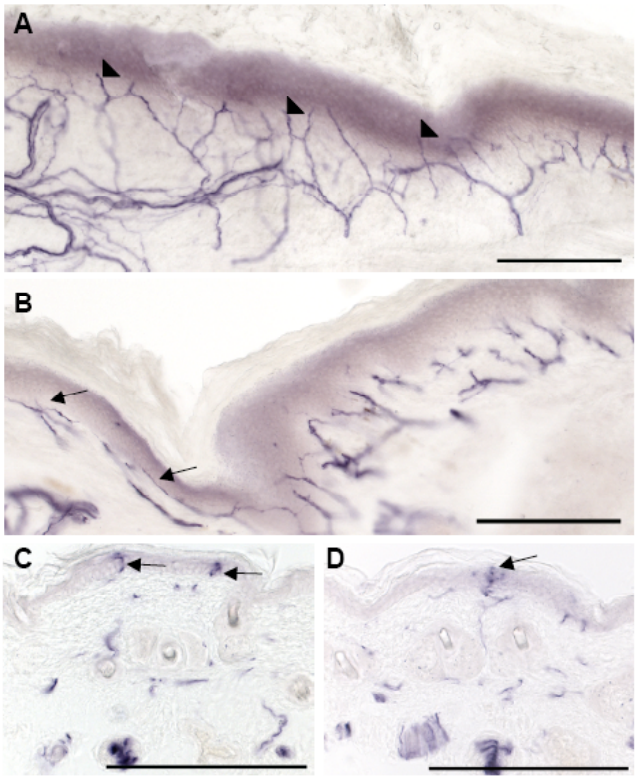
A
B
C
D

Figure 3. Calcium imaging of capsaicin responsiveness in cultured TRPV1$^{PLAP\text{-}nlacZ}$ DRG neurons.

(A-C) Cultured DRG neurons from 6 week old mice were imaged with Fura-2-AM dye (A) at background, and following stimulation with (B) 1μM capsaicin, and (C) high K^+ Ringer's solution.

(D) Cells were then fixed and stained for nlacZ expression.

(E) 340/380 ratios of cells as numbered in D. Scale bar = 100μm.

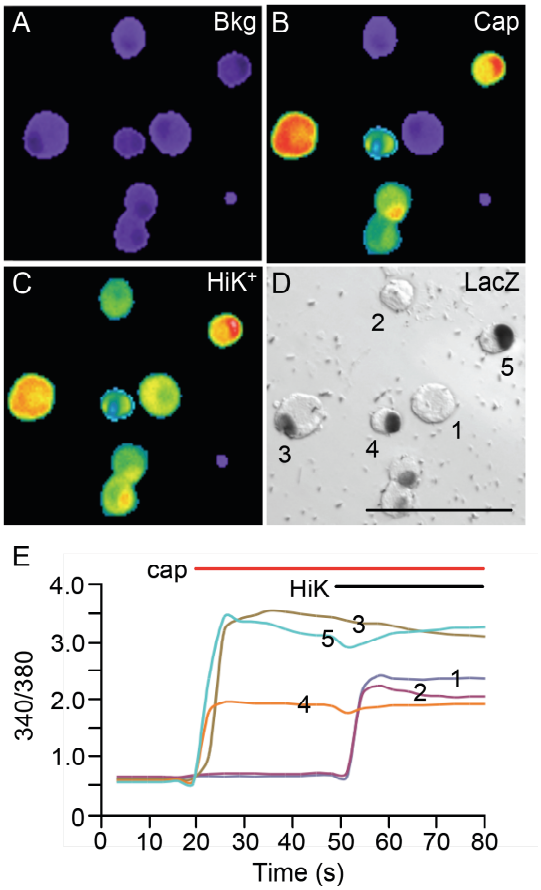
A
Bkg
B
Cap
C
HiK+
D
LacZ
1
2
3
4
5
E
cap
HiK
340/380
4.0
3.0
2.0
1.0
0
0
10
20
30
40
50
60
70
80
Time (s)

Figure 4. Double labeling of DRG neurons with nlacZ and markers of primary afferent neuron populations.

(A-E) Left panel show DRG sections stained for nlacZ expression with the x-gal reaction (pseudocolored magenta). Center panel shows the same sections stained by immunohistochemistry for the markers listed. Right panel shows merged images.

(F-G) DRG section stained for nlacZ expression with (F) 1 d and (G) 3d exposure to x-gal reaction solution. Scale bar = 100μm.

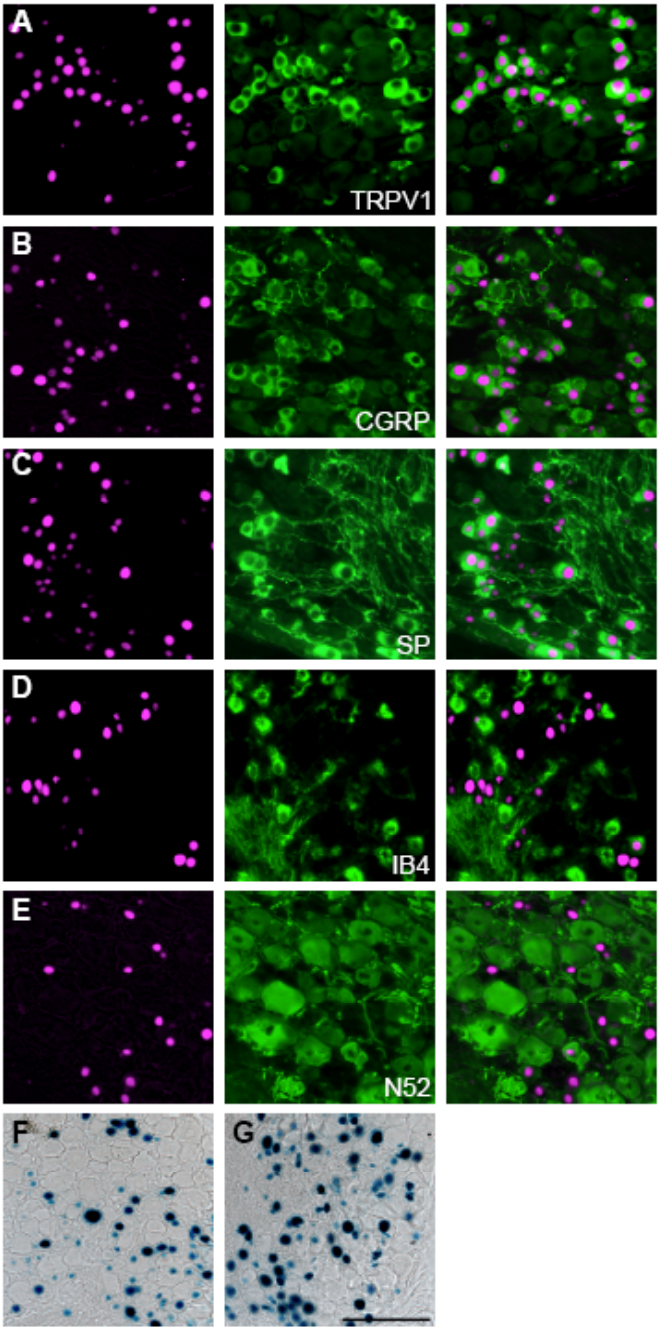
A
TRPV1
B
CGRP
C
SP
D
IB4
E
N52
F
G

Figure 5. Developmental timecourse of nlacZ staining in DRG.

(A-E) nlacZ staining on 20 μm sections of mouse embryo.

(A) No nlacZ staining is observed at e11.5 (Dotted lines delineate DRGs).

(B) By e12.5, a small minority of DRG cells is $nlacZ^+$. Inset shows magnification of boxed area. Note $nlacZ^+$ cells (arrows) .

(C-E) nlacZ expression increases from e13.5 to e14.5, when the percentage of labeled cells reaches a maximum. By e16.5, the overall percentage of $nlacZ^+$ cells has dropped slightly, but staining intensity within individual cells is increased. Scale bar = 200μm.

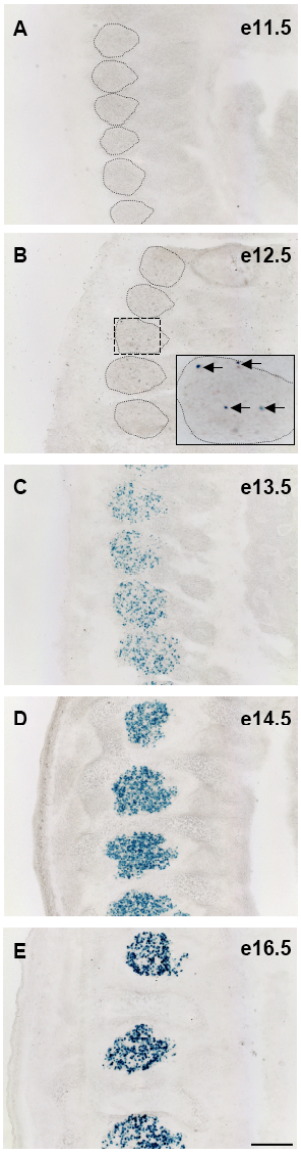
A
e11.5
B
e12.5
C
e13.5
D
e14.5
E
e16.5

Figure 6. Brain expression of PLAP.

(A) PLAP staining in nucleus caudalis of the medulla (arrow) and the nucleus of the solitary tract (arrowhead).

(B) Robust PLAP staining in the solitary tract (arrow).

(C) PLAP staining in the ventral medulla (inset shows magnification of boxed area, near nucleus ambiguus).

(D) PLAP+ axons in the granule layer of the olfactory bulb (inset shows magnification of boxed area).

(E) External lateral parabrachial nucleus receives extensive $PLAP^+$ innervation (arrow).

(F) $PLAP^+$ fibers extend throughout the parabrachial nucleus (arrows). Inset shows magnification of boxed area. Scale bars = 500μm.

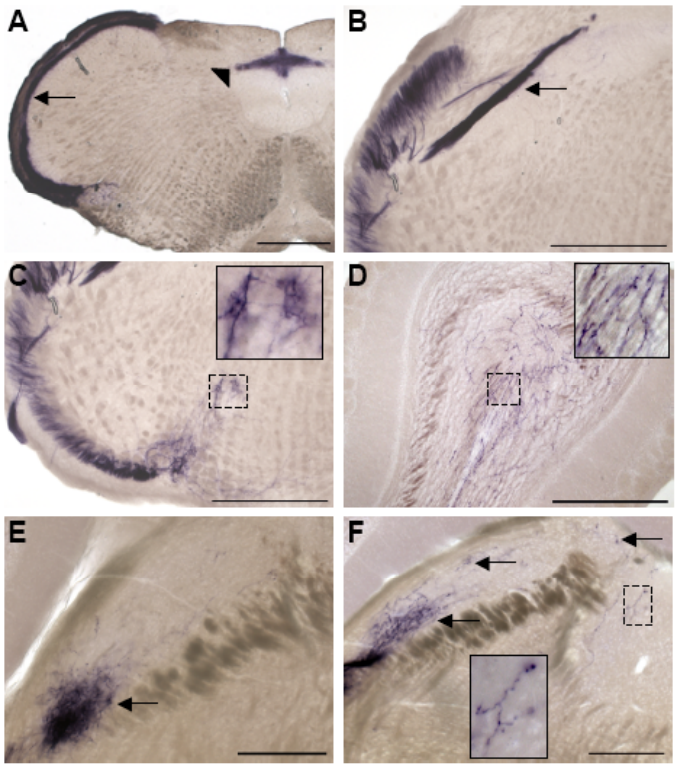
A
B
C
D
E
F

Figure 7. Brain expression of nlacZ.

Sparse nlacZ expression was observed in (A) PAG and (B) interpeduncular nucleus. More robust nlacZ staining was seen in (C) arcuate nucleus of the hypothalamus and (D) accessory olfactory bulb.

(E-F) nlacZ labeled a discrete subset of hippocampal neurons, that co-labeled for reelin, a marker of Cajal-Retzius cells. In F, x-gal reaction product is pseudocolored magenta, and reelin is green.

(G) RT-PCR analysis fails to show evidence of TRPV1 mRNA in brain regions with nlacZ staining, but demonstrates TRPV1 mRNA in TG and cremaster muscle. OB = olfactory bulb; Co = cortex; Hi = hippocampus; Ar = arcuate; In = interpeduncular nucleus; PG = periaqueductal gray; Ce = cerebellum; SC = spinal cord; TG = trigeminal ganglion; Li = liver; Bl = bladder; Cr = cremaster; neg = no cDNA. Scale bars in A-E = 500μm, in F = 100μm.

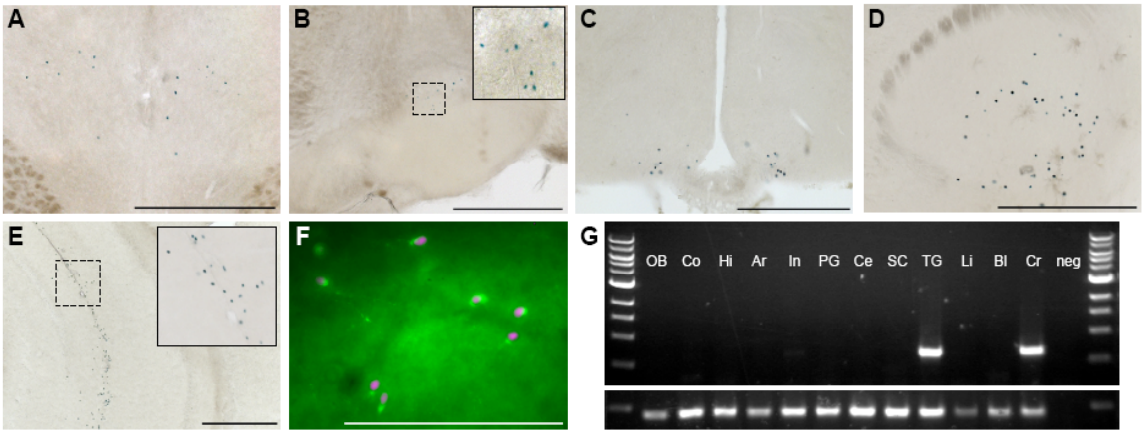
A
B
C
D
E
F
G
OB Co Hi Ar In PG Ce SC TG Li Bl Cr neg

Figure 8. Evidence of TRPV1 expression in a subset of arteriolar smooth muscle cells.

(A) PLAP staining in cremaster muscle.

(B) nlacZ staining in cremaster muscle.

(C) Whole mount nlacZ stain of TG, showing TRPV1 cell bodies (arrowhead) and presumptive smooth muscle cell staining (arrow).

(D) nlacZ staining in whole mount of ear.

(E) nlacZ staining in section of tongue.

(F) nlacZ in tongue (pseudocolored magenta) co-localizes with staining for smooth muscle actin (green). Inset shows magnification of boxed area.

(G) PLAP staining of whole mount paw skin shows presumptive smooth muscle cell staining (arrows) as well as axonal label.

(H) PLAP staining in whole mount of trachea, showing smooth muscle label (arrows). Scale bars in A-D, G-H = 500μm, in E-F = 100μm.

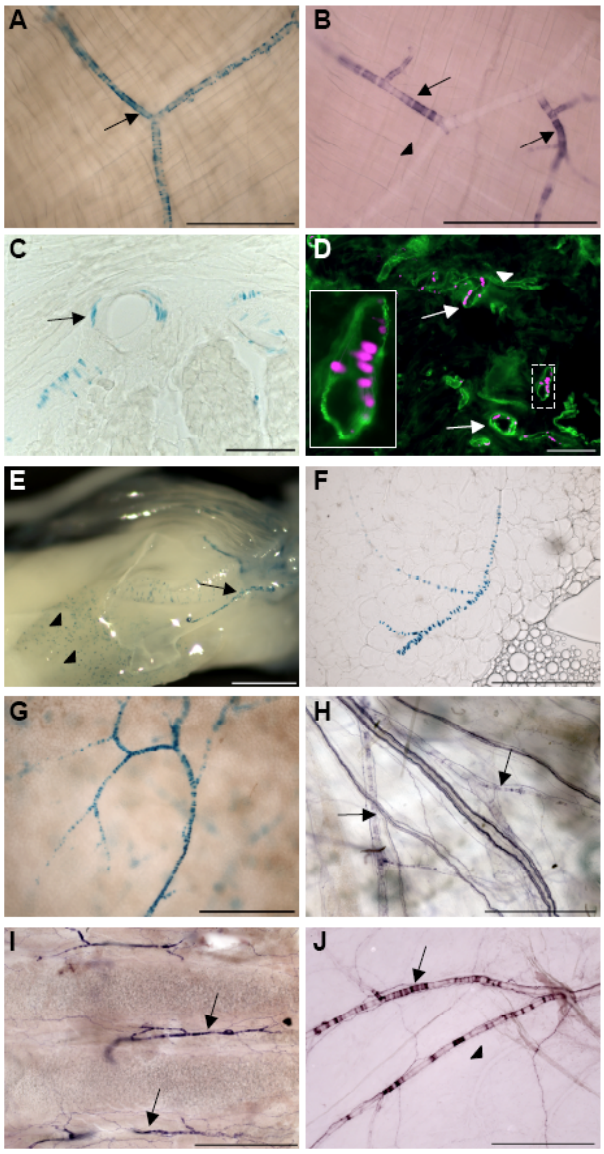
A
B
C
D
E
F
G
H
I
J

Figure 9. Reduction of PLAP staining in brain and nlacZ staining in smooth muscle cells following systemic resiniferatoxin injection.

(A-D) Systemic resiniferatoxin injection eliminates PLAP staining in (A) trigeminal ganglion, (B) caudal medulla, (C) parabrachial nucleus and (D) olfactory bulb. Images on the left show PLAP staining in vehicle-treated mice, and images on the right show PLAP staining in resiniferatoxin-treated mice .

(E-F) nlacZ staining of smooth muscle cells is greatly reduced in (E) the tongue and (F) the ear following resiniferatoxin treatment. Images of the left show nlacZ staining in vehicle-treated mice, and images on the right show nlacZ staining in resiniferatoxin-treated mice.

Scale bars = 200μm in A-E and 500μm in F.

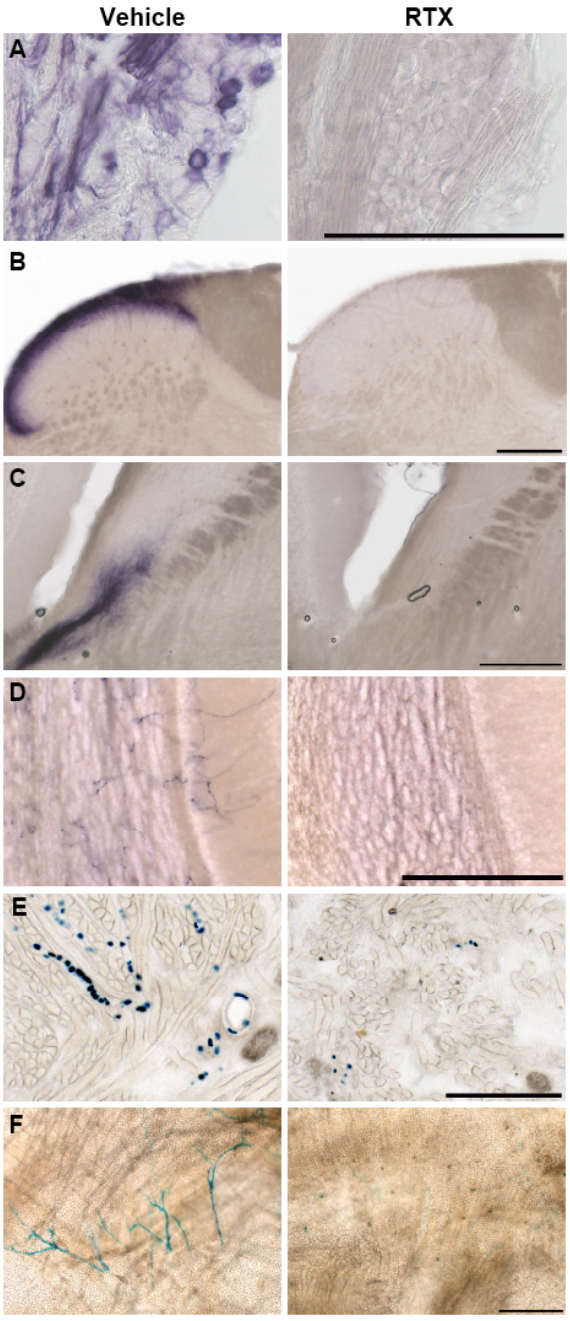
Vehicle
RTX
A
B
C
D
E
F

Supplemental Figure S1. PLAP staining in spinal cord is eliminated by intrathecal capsaicin injection and reduced by axotomy.

(A) PLAP staining in spinal cord of vehicle-treated mouse.

(B) PLAP staining is eliminated following intrathecal injection of 10μg capsaicin.

(C) PLAP staining is significantly reduced following complete sciatic nerve transection. Note the selective loss PLAP+ fibers in the medial aspect of the spinal cord (arrows), where sciatic nerve afferents terminate.

Scale bars = 200μm.

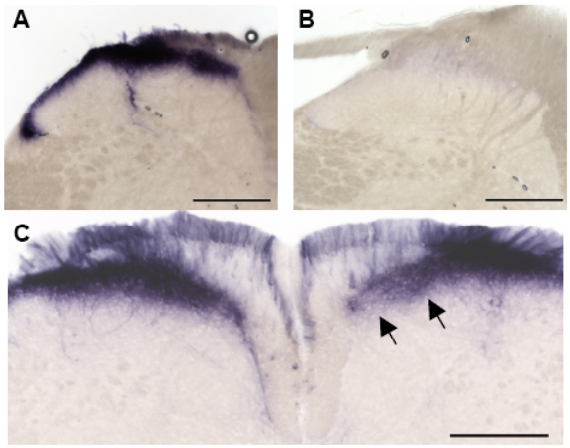
A
B
C

Supplemental Figure S2. nlacZ shows substantial overlap with IB4 in nodose ganglion.

(A-C) 14 μm section of nodose ganglion stained for (A) βgal immunoreactivity (to visualize nlacZ) and (B) IB4 binding. A merged image is shown in C. Arrowheads point to double-labeled cells. Scale bar = 100 μm.

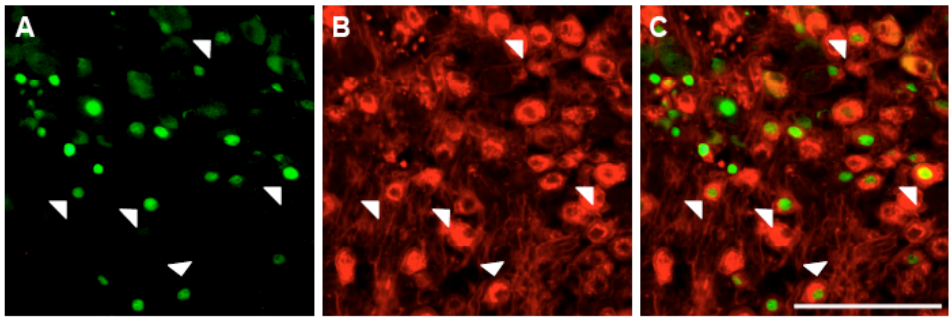
A
B
C

Supplemental Figure S3. PLAP staining in parabrachial nucleus overlaps with $CGRP^+$ cells.

(A) Dense $PLAP^+$ fibers in parabrachial nucleus overlaps with (B) $CGRP^+$ cell bodies, which mark the external lateral region of the parabrachial nucleus. A merged image is shown in C. Scale bar = 200 μm.

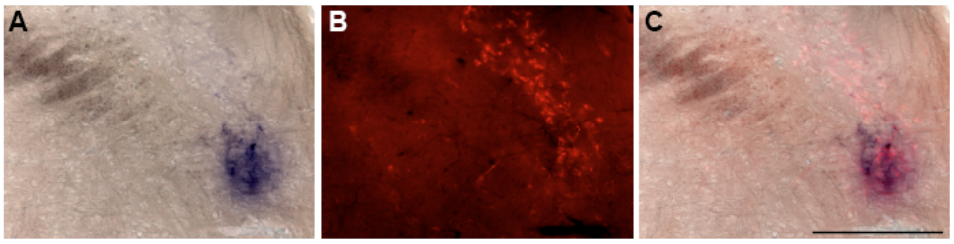
A
B
C

Chapter 4

Distinct subsets of unmyelinated primary sensory fibers mediate behavioral responses to noxious thermal and mechanical stimuli

Daniel J. Cavanaugh[1], Hyosang Lee[2], Liching Lo[2], Shannon D. Shields[1], Mark J. Zylka[3], Allan I. Basbaum[1] and David J. Anderson[2]

[1]Department of Anatomy, University of California, San Francisco, San Francisco CA 94158, [2]Division of Biology 216-76 and Howard Hughes Medical Institute, California Institute of Technology, Pasadena CA 91125, and [3]Department of Cell and Molecular Physiology, University of North Carolina, Chapel Hill NC 27559

The text of this chapter is a reprint of the material as it appears in the Proceedings of the National Academy of Sciences of the USA:
Proc Natl Acad Sci U S A. 2009 Jun 2;106(22):9075-80.

Abstract

Behavioral responses to painful stimuli require peripheral sensory neurons called nociceptors. Electrophysiological studies show that most C-fiber nociceptors are polymodal, i.e. respond to multiple noxious stimulus modalities, such as mechanical and thermal; nevertheless these stimuli are perceived as distinct. Therefore, it is believed that discrimination between these modalities only occurs at spinal or supraspinal levels of processing. Here we provide evidence to the contrary. Genetic ablation in adulthood of unmyelinated sensory neurons expressing the G protein-coupled receptor, Mrgprd, reduces behavioral sensitivity to noxious mechanical, but not to heat or cold, stimuli. Conversely, pharmacological ablation of the central branches of TRPV1$^+$ nociceptors, which constitute a non-overlapping population, selectively abolishes noxious heat pain sensitivity. Combined elimination of both populations yielded an additive phenotype with no additional behavioral deficits, ruling out a redundant contribution of these populations to heat and mechanical pain sensitivity. This double-dissociation suggests that the brain can distinguish different noxious stimulus modalities from the earliest stages of sensory processing.

Introduction

Nociceptors are heterogeneous by a variety of molecular criteria (Snider and McMahon, 1998; Julius and Basbaum, 2001; Dong et al 2001, Braz et al 2005), but the functional significance of this heterogeneity is unclear. Electrophysiological recordings of unmyelinated primary afferent (C) fibers from dorsal root ganglia (DRG) show that most (>70%) nociceptors are polymodal: they can be activated by multiple types of painful stimuli, such as mechanical or thermal (Perl, 1996; Cain et al, 2001; Lawson et al, 2008). This has led to a prevailing view that the brain's ability to discriminate different noxious stimulus modalities is unlikely due to modality-specific primary nociceptor subsets. Rather, it is believed that modality discrimination occurs by the decoding of nociceptor inputs in higher-order spinal cord or brain areas (Melzack and Wall, 1962; Perl, 2007). A prediction of this hypothesis is that targeted ablation of any one specific nociceptor subpopulation should cause deficits in behavioral responses to noxious stimuli of multiple modalities. Indeed, some previous studies, using genetic- or immunotoxin-based methods, support this prediction (Vulchanova et al, 2001; Tarpley et al, 2004; Abrahamsen et al, 2008).

A critical issue in such experiments, however, regards the cellular specificity and timing of administration of the markers/reagents used for ablation. For example, if ablation of a population of DRG neurons using a given marker caused deficits in behavioral sensitivity to multiple pain modalities (Vulchanova et al, 2001; Tarpley

et al, 2004; Abrahamsen et al, 2008), it could reflect the expression of this marker either in a homogeneous population of polymodal nociceptors, or in multiple, modality-specific, subpopulations. Modality specificity of nociceptor subpopulations could also be difficult to detect if ablation is performed constitutively using markers which, although specific in adulthood, are transiently expressed more broadly during development (Molliver et al, 1997).

We have examined the behavioral consequences of selectively eliminating two non-overlapping subsets of nociceptors, based on their expression of specific receptors, in the adult. Genetic ablation of neurons that express the sensory neuron-specific, G protein-coupled receptor, Mrgprd (Dong et al, 2001; Zylka et al, 2005), caused specific deficits in the behavioral response to noxious mechanical, but not to noxious heat or cold, stimuli. Conversely, eliminating the central projections of neurons that express the heat sensitive channel, TRPV1 (Caterina et al, 1997), caused a complete loss of heat pain sensitivity, without affecting responses to noxious mechanical or cold stimuli. Combined elimination of both populations yielded an additive phenotype with no further behavioral deficits. These data reveal the existence of distinct subsets of primary sensory neurons that selectively mediate behavioral responses to different noxious stimulus modalities.

Results

Conditional ablation of Mrgprd$^+$ nociceptors

Mrgprd$^+$ afferents exclusively innervate the epidermis, and constitute >90% of all non-peptidergic cutaneous C-fibers (Dong et al, 2001; Zylka et al, 2003; Zylka et al, 2005). These neurons bind isolectin IB4 and terminate in inner lamina II of the spinal cord dorsal horn (Snider and McMahon, 1998). In vitro, Mrgprd$^+$ neurons exhibit electrophysiological properties characteristic of nociceptors (Dussor et al, 2008), and behave as C-polymodal units in *ex vivo* recordings (Rau et al, 2009).

To determine the behavioral consequences of ablating Mrgprd$^+$ neurons, we used a conditional strategy (Saito et al, 2001; Luquet et al, 2005), in which the human diphtheria toxin receptor (DTR) was inserted in the *Mrgprd* locus (Fig. 1A) by homologous recombination in murine embryonic stem cells. The human DTR binds diphtheria toxin (DTX) with 10^5-fold higher affinity than does the endogenous mouse receptor. Heterozygous *Mrgprd$^{DTR/+}$* mice (hereafter referred to as *Mrgprd^{DTR}* mice) expressed DTR in an identical pattern as a GFP reporter expressed from a second targeted *Mrgprd* allele (Fig. 1B-D). Injection of DTX into adult *Mrgprd^{DTR}* mice produced a virtually complete (>98%) loss of Mrgprd$^+$ cell bodies in the DRG (Fig. 1E, F), and of their central and peripheral fibers (Fig. 1I-N). Consistent with Mrgprd expression in the non-peptidergic afferents, DTX treatment caused an 82.4% reduction in labeling for IB4, but no change in labeling for calcitonin gene-related peptide (CGRP), a marker of peptidergic afferents (Fig. 1E-N and Supplemental Table 1). The overall reduction in neuron number is commensurate with the size of the Mrgprd$^+$ population, suggesting that

no other population is affected. No loss of Mrgprd$^+$ neurons in the DRG was observed in mice without DTX injection (Fig. 1B-D and Supplemental Table 1). *Mrgprd^{DTR}* mice were normal in viability, overall appearance and body weight, both before and after DTX treatment.

Selective reduction of behavioral responses to noxious mechanical stimuli following ablation of Mrgprd$^+$ neurons

To determine the behavioral consequences of ablating Mrgprd$^+$ neurons, we measured paw withdrawal responses to calibrated von Frey filaments. Prior to DTX treatment, the mechanical threshold of *Mrgprd^{DTR}* mice was not different from that of WT littermates (Fig. 2A). Following DTX, however, the mechanical threshold of Mrgprd^{DTR} mice doubled (from 0.41±.04 to 0.99±.15 g; Fig. 2A; p<.01). There was no significant change in WT mice after DTX treatment (Fig. 2A). The elevated mechanical threshold in *Mrgprd^{DTR}* mice persisted for at least 31 days after DTX (not shown). The response frequency to a series of von Frey filaments ranging from 0.16-1.4 g was also significantly reduced in DTX-treated *Mrgprd^{DTR}* mice, relative to controls (Fig. S1). These data demonstrate that Mrgprd$^+$ neurons are necessary for normal responsiveness to acute, noxious mechanical stimuli. Importantly, no deficits in mechanical pain sensitivity were detectable in mice in which Mrgprd$^+$ neurons were deleted from birth (Fig. S2, S3), suggesting that other nociceptor populations can functionally compensate for the loss of Mrgprd$^+$ neurons, but only if the loss occurs sufficiently early in development (Luquet et al, 2005).

We next asked whether Mrgprd^{+} afferents also contribute to the mechanical hypersensitivity caused by hindpaw injection of an inflammatory mediator, Complete Freund's Adjuvant (CFA). The mechanical thresholds of DTX-treated *Mrgprd^{DTR}* mice were significantly higher than DTX-treated WT mice at all time points following CFA injection (Fig. 2B; $p<.01$). In control (DTX-treated WT) mice, mechanical thresholds dropped significantly 1 day following CFA, to 40% of baseline (Fig. 2C, $p<.05$), and recovered to pre-CFA baseline by day 3 (Fig. 2B; $p<.01$). In contrast, the mechanical threshold in DTX-treated *Mrgprd^{DTR}* mice at 1 day after CFA treatment was only reduced to 80% of pre-CFA values. Thus, Mrgprd^{+} neurons are required for full expression of mechanical hypersensitivity after tissue injury.

Behavioral responses to noxious heat and cold stimuli are normal in DTX-treated *Mrgprd^{DTR}* mice

Strikingly, DTX-treated *Mrgprd^{DTR}* mice exhibited no deficits in their behavioral sensitivity to noxious heat, as scored by tail withdrawal latency from a hot water bath (Fig. 2D), latency to exhibit evidence of discomfort (paw shaking and licking) on a hot plate (Fig. 2E), or latency to paw withdrawal from radiant heat (Fig. 2F, BL). Following CFA injection, DTX-treated *Mrgprd^{DTR}* and WT mice developed equivalent heat hypersensitivity (Fig. 2F). Thus, Mrgprd^{+} neurons are dispensable for both baseline heat pain sensitivity, as well as for CFA-induced sensitization to heat pain, *in vivo.*

We next evaluated cold sensitivity in the DTX-treated *Mrgprd*^{DTR} mice. In a test of temperature preference between a 32^{o}C chamber and a chamber at variable cold temperatures (20 to 5^{o}C), both DTX-treated WT and *Mrgprd*^{DTR} mice preferred the 32^{o}C chamber (Fig. S4A). Furthermore, DTX-treated WT and *Mrgprd*^{DTR} mice exhibited identical paw withdrawal latencies on a -5^{o}C plate (Fig. S4B). Taken together, these results indicate that Mrgprd^{+} neurons are not required for normal cold sensitivity.

The lack of a requirement for Mrgprd^{+} neurons in behavioral responses to noxious heat was surprising, given their polymodal properties. To investigate whether ablation of Mrgprd^{+} neurons might be compensated by other heat-sensitive nociceptor populations, we sought to ablate a known heat-sensitive C-fiber population, while sparing Mrgprd^{+} neurons. We therefore focused on the large population of TRPV1^{+} nociceptors (Caterina and Julius, 2001). Previous studies indicated that pharmacological ablation of TRPV1^{+} afferents causes at least a partial loss of heat pain sensitivity (Yaksh et al, 1979; Gamse, 1982; Holzer, 1991). Furthermore, less than 10% of Mrgprd^{+} neurons express TRPV1 *in vivo* (Dong et al, 2001; Zylka et al, 2005), and no more than 10% respond to the TRPV1 agonist capsaicin *in vitro* (Dussor et al, 2008). TRPV1^{+} and Mrgprd^{+} neurons are therefore largely non-overlapping.

Ablation of the central terminals of TRPV1^{+} afferents

Because TRPV1 is also expressed in cells outside of the DRG (Caterina, 2003) we could not use the DTR strategy to selectively eliminate TRPV1$^+$ nociceptors. Instead, we exploited the fact that high doses of capsaicin destroy TRPV1$^+$ fibers. Intrathecal injection of capsaicin eliminated TRPV1$^+$ afferent fibers in the lumbar spinal cord (Fig. 3A, E), however, TRPV1 staining of DRG cell bodies was preserved (Fig. S5A-D). Importantly, capsaicin injection also eliminated retrograde transport of fluorogold from the spinal cord to the cell bodies of TRPV1$^+$ neurons (Fig. S5A-C), indicating that the loss of TRPV1 fiber staining reflected destruction of the central terminals of the TRPV1$^+$ nociceptors, not simply downregulation of TRPV1 expression.

The pharmacological ablation of TRPV1$^+$ afferents spared the Mrgprd$^+$ afferent population, as revealed by the preserved expression of a GFP reporter included in the DTR targeting cassette (Fig. 1A, 3F). Consistent with this, IB4 binding was unchanged (Fig. 3C, E). In contrast, there was a significant reduction in the expression of CGRP, which is found in many TRPV1$^+$ neurons, to 54.5±5.0% of vehicle-treated controls (p=.0004; Fig. 3B, E). Immunoreactivity for other markers of TRPV1 afferents was also reduced in the spinal cord (viz. the 5HT1D subtype of serotonin receptor (Potrebic et al, 2003), and the water channel, aquaporin 1 (Shields et al, 2007) Fig. S6A, B, and E). Importantly, we found no change in immunoreactivity for the substance P receptor (NK1), a marker of spinal cord lamina I projection neurons that are postsynaptic targets of TRPV1$^+$ afferents, or for calbindin, which marks a large population of spinal cord interneurons (Fig.

S6C-E). These observations indicate that capsaicin treatment did not produce a generalized neurotoxic effect in the spinal cord.

Intrathecal capsaicin treatment eliminates behavioral responses to noxious heat

Capsaicin-treated mice showed a complete and prolonged behavioral insensitivity to heat (Fig. 4A, B). When tested on a 55^{o}C hotplate, vehicle-treated mice licked their hindpaw with a latency of 11.8±.8 s, whereas capsaicin-treated mice were unresponsive up to the 30 s cut-off (p<.0001). Consistent with these behavioral data, capsaicin treatment eliminated induction of Fos, a marker of neuronal activity, in the dorsal horn of the spinal cord following hindpaw exposure to a 55^{o}C stimulus (Fig. 4E, F). Capsaicin-treated mice also showed no withdrawal of the hindpaw in response to radiant heating (p<.0001; Fig. 4C, BL), and did not discriminate between 30^{o}C and 45^{o}C in the temperature preference assay, while control mice strongly preferred 30^{o}C (Fig. 4D; p=.008).

TRPV1^{+} fiber ablation also affected both the induction and maintenance of behavioral heat hypersensitivity following CFA injection. In vehicle-treated mice, CFA injection produced a profound heat hypersensitivity that returned to baseline over the course of 3 days. In contrast, mice pre-treated with capsaicin 1 week prior to CFA injection were not only unresponsive to heat before the inflammation was induced, but also showed no change in sensitivity following CFA (Fig. 4C). Even when mice were treated with capsaicin 1 day after CFA injection, they

completely lost sensitivity to noxious heat (p<.0001). Thus ablation of TRPV1$^+$ fibers abolishes all heat pain sensitivity, under both normal conditions and in the setting of injury.

The complete loss of heat responsiveness following intrathecal capsaicin indicates that Mrgprd$^+$ neurons are unable to compensate for the absence of TRPV1$^+$ afferents. These results also indicate that other heat-sensitive nociceptors, such as those that express the capsaicin-insensitive heat channel TRPV2 (Caterina et al, 1999; Lewinter et al, 2004), cannot compensate either. Capsaicin-treatment caused no change in TRPV2 staining (p=.21; Fig. 3D, E), confirming that TRPV2$^+$ neurons are spared by this manipulation.

Behavioral responses to mechanical and cold stimuli are normal in capsaicin-treated mice

Capsaicin treatment did not influence behavioral responses to either mechanical or cold stimuli. The mechanical withdrawal threshold in capsaicin-treated mice did not differ from that of vehicle-treated mice (p=.47; Fig. 4G). Furthermore, CFA-induced mechanical hypersensitivity persisted in mice treated with capsaicin either before or after CFA injection (Fig. 4H). Although treatment with capsaicin prior to CFA injection caused a slight reduction in mechanical hypersensitivity at 1 day post CFA (Fig. 4H; p=.0001), treatment with capsaicin after CFA injection had no effect on mechanical hypersensitivity. Thus, TRPV1$^+$ afferents are not required for mechanical hypersensitivity following injury, but may facilitate the

initial development of hypersensitivity, perhaps by modulating other populations of mechanoreceptive neurons.

Capsaicin-treated mice also exhibited normal cold pain sensitivity, as assessed by hindpaw withdrawal latency on a –5^{o}C plate (Fig. S4C) and discrimination between 30 and 20^{o}C in the temperature preference test (Fig. 4D). Thus, the perception of both moderate and intense cold as aversive/painful is preserved in the absence of input carried by TRPV1^{+} nociceptors. As the TRPA1 channel is found in a subset of TRPV1 afferents (Story et al, 2003), this result is consistent with our conclusion that TRPA1 is not required for acute cold-evoked pain behavior (Bautista et al, 2006).

Combined ablation of Mrgprd and TRPV1-expressing nociceptors does not produce further deficits

TRPV1^{+} afferents were not sufficient to support full mechanical sensitivity in the absence of Mrgprd neurons^{+}. Nevertheless, the partial loss of mechanical pain sensitivity in DTX-treated *Mrgprd*^{DTR} mice left open the possibility that TRPV1^{+} afferents contribute to the residual mechanical sensitivity in these mice. To address this possibility, we compared mechanical sensitivity in DTX-treated *Mrgprd*^{DTR} mice, before and after ablation of TRPV1^{+} afferents.

Importantly, capsaicin treatment in mice lacking Mrgprd^{+} neurons produced no further decrease in mechanosensitivity, compared to that observed prior to

capsaicin treatment (Fig. 5B; 1.05±.38 g before and 0.87±.22 g after capsaicin-treatment; p=.315). As expected, the heat sensitivity of DTX-treated *Mrgprd*^{DTR} mice was fully eliminated following capsaicin treatment (Fig. 5A, p<.001), confirming the efficacy of TRPV1^{+} fiber ablation. Thus, TRPV1^{+} neurons do not contribute to the residual mechanical pain sensitivity in *Mrgprd*^{DTR}/DTX mice. This residual sensitivity must therefore reflect a contribution of the remaining TRPV1^{-} and Mrgprd^{-} cutaneous C fibers, and/or of myelinated afferents (e.g., high-threshold mechanosensitive Aδ fibers).

Discussion

Genetic approaches to nociception have focused primarily on identifying individual molecules that transduce painful stimuli. However, the discrimination of different pain modalities by the brain depends not only on which molecules are activated, but also on which neurons. Primary afferent nociceptors are heterogeneous, and therefore an understanding of the behavioral function of different subsets of these neurons is essential to deciphering the logic by which different types of painful stimuli are sensed and encoded. Here we selectively ablated two non-overlapping populations of nociceptors, and observed a double dissociation between noxious mechanical and heat pain sensitivity. These data suggest that behavioral discrimination between different pain modalities can occur at the earliest stages of sensory processing.

A caveat is that our behavioral observations are constrained by test cut-off and intensity limitations that are necessary in order to prevent tissue damage. Therefore, we cannot exclude that these nociceptor classes contribute to behavioral responses to both heat and mechanical stimuli, but only at stimulus intensities greater than those we tested. Furthermore, because mechanical pain sensitivity is only partially reduced in mice lacking Mrgprd$^+$ neurons, our results do not rule out the existence of Mrgprd$^-$ subpopulations of mechanosensitive nociceptors that also mediate behavioral responses to other noxious stimulus modalities.

Mrgprd$^+$ neurons are selectively required for painful mechanosensation

Our data indicate that Mrgprd$^+$ neurons are necessary for full behavioral sensitivity to noxious mechanical but not thermal stimuli. The lack of a heat pain deficit in mice lacking these neurons cannot be explained by either redundancy or compensation, because all heat-pain sensitivity is lost in mice that lack TRPV1$^+$ afferents, but which retain nearly all Mrgprd$^+$ neurons. Nevertheless, it is possible that Mrgprd$^+$ neurons contribute to heat pain sensitivity in intact animals, in a manner dependent on TRPV1$^+$ neurons.

Previous studies have reported that ablation of IB4$^+$ neurons (which include all Mrgprd$^+$ neurons) using an IB4-saporin conjugate transiently reduced both mechanical and heat pain sensitivity (Vulchanova et al, 2001; Tarpley et al, 2004), in contrast to the selective and prolonged mechanosensitive deficit in mice

lacking Mrgprd$^+$ neurons. However, IB4-saporin targets a carbohydrate epitope present on multiple cell types, whereas Mrgprd is exclusively expressed in unmyelinated afferents (Dong et al, 2001; Zylka et al, 2005). Moreover, the IB4-saporin experiments were performed in the rat, in which IB4 labels a more heterogeneous population of neurons than does Mrgprd in the mouse (Price et al, 2007). Therefore, the cellular specificity afforded by targeted ablation of Mrgprd$^+$ neurons in the mouse is much greater than that achieved by ablation of IB4$^+$ neurons in the rat. Whether different species of rodent exhibit different degrees of nociceptor specialization is an interesting question for future investigation. The recent observation that pharmacological manipulation of TRPV1 channels in rat affects mechanical as well as heat sensitivity (Binshtok et al, 2007) suggests either that the neurons that express these channels include mechanosensitive nociceptors in that species, or that such nociceptors can be non-cell-autonomously influenced by manipulation of heat-sensitive nociceptors.

Abrahamsen *et al* recently reported that genetic ablation of nociceptors that express the Nav1.8 sodium channel, which include most IB4$^+$ neurons, caused profound deficits in basal mechanical and cold pain sensitivity, as well as inflammatory pain deficits (Abrahamsen et al, 2008). In contrast, ablation of Mrgprd$^+$ neurons (which constitute ~90% of IB4$^+$ cutaneous afferents) impaired mechanical but not cold pain sensitivity. It is likely that elimination of Nav1.8$^+$ DRG neurons leads to changes in the behavioral response to multiple modalities because this channel is present in >85% of small-diameter neurons, including

both Mrgprd$^+$ and TRPV1$^+$ neurons. By contrast, the manipulations used in the present study target more specific populations of neurons, and reveal more specific phenotypes.

TRPV1$^+$ neurons are essential for heat-pain sensitivity

Ablation of TRPV1$^+$ central afferent fibers by capsaicin injection abolished heat-pain sensitivity, without affecting the responses to noxious mechanical or cold stimulation. Previous studies using similar approaches reported less complete deficits in heat pain sensitivity than we observed here, but the effects were also modality-specific (Yaksh et al, 1979; Gamse, 1982; Fitzgerald and Woolf, 1982; Holzer, 1991; Karai et al, 2004). The partial behavioral deficits observed in earlier studies using capsaicin or resiniferatoxin treatment likely reflected incomplete ablation of the TRPV1$^+$ afferent fibers, as these studies were performed prior to the availability of reagents to monitor TRPV1 expression.

It is surprising, given our results, that Abrahamsen *et al* observed only subtle deficits in heat pain sensitivity following ablation of Nav1.8$^+$ neurons, since this manipulation destroyed a large fraction of TRPV1$^+$ neurons. This may reflect compensation by the small fraction of TRPV1$^+$ neurons that were spared. Alternatively, the fact that Nav1.8$^+$ neurons were constitutively ablated from the embryonic stage at which this gene is first transcribed (Abrahamsen et al, 2008) could permit compensation by other neuronal populations during development

and maturation, as we observed following constitutive ablation of Mrpgrd^{+}neurons (Fig. S2, S3).

The complete heat pain-insensitivity of mice lacking central TRPV1^{+} fibers contrasts with the phenotype of *Trpv1* knockout mice, which exhibit only a partial reduction in heat sensitivity (Caterina et al, 2000; Davis et al, 2000). The residual heat pain behavior in these gene knockout mice must, therefore, reflect the existence of additional molecular heat transducers that act, either cell-autonomously or non-autonomously, via TRPV1^{+} neurons.

Physiology vs. behavior

How do we reconcile our behavioral observations with the fact that the majority of C fibers are polymodal by electrophysiological criteria (Lawson et al 2008)? It is possible that the response properties of these nociceptors, as determined by *ex vivo* electrophysiological recordings, differ from those exhibited by these neurons *in vivo*. Alternatively, Mrgprd^{+} and TRPV1^{+} neurons may indeed be activated by both heat and mechanical stimuli *in vivo*, but these two types of stimulus modalities may evoke different spiking patterns within each class of nociceptors (for example, see Stucky and Lewin, 1999). If so, then perhaps only one “preferred” modality is able to activate each nociceptor subtype to a level sufficient to drive second-order spinal cord neurons above a threshold required to evoke nocifensive behavior. It is also possible that these nociceptor subtypes convey polymodal information to the spinal cord, but that this information

contributes to aspects of the pain experience that are not measurable by the behavioral assays we used. Electrophysiological recordings from spinal cord neurons of mice lacking Mrgprd$^+$ or TRPV1$^+$ afferents should help to resolve these questions. Finally, although polymodal nociceptors predominate, DRG neurons that are modality-specific by electrophysiological criteria do exist. For example, a recent electrophysiological study described a heat-selective subpopulation of nociceptors, all of which expressed TRPV1 (Lawson et al, 2008). Our data suggest that this population is likely to be particularly relevant for heat-evoked behavioral responses.

TRPV1$^+$ and Mrgprd$^+$/IB4 fibers target distinct laminae in the dorsal horn of the spinal cord (Snider and McMahon, 1998), innervate different layers of the epidermis (Zylka et al, 2005), and likely engage distinct ascending circuits (Braz et al, 2005) (Fig. 5C). These parallel pathways, therefore, represent a neuroanatomical substrate for the behaviorally relevant processing of different pain modalities by these two classes of peripheral nociceptors. Whether these pathways exclusively mediate mechanical vs. heat pain discrimination, or have additional functions, is not clear. Whatever the case, our data suggest that this discrimination can be achieved at the earliest stages of nociceptive sensory processing and does not, as previously believed, exclusively emerge at spinal or supraspinal levels. Thus, as in the mammalian (Chandrashekar et al, 2006) and invertebrate (Scott, 2005) gustatory systems, the cellular logic of information processing in the “pain” system incorporates distinct subsets of primary sensory

cells that selectively mediate appropriate behavioral responses to different stimulus modalities.

Experimental Procedures

Animals and Injections

Animal experiments were approved by the Institutional Animal Care and Use Committee and conducted in accordance with the NIH Guide for the Care and Use of Laboratory Animals and the recommendations of the International Association for the Study of Pain. Animals were housed 2-5 per cage and maintained on a 12h light/dark schedule in a temperature-controlled environment with ad lib access to food and water. DTX (100 μg/kg) was injected intraperitoneally on 2 days, separated by 72 hours. Behavioral tests were performed 7 to 31 days after the first DTX injection. For intrathecal capsaicin studies, adult male C57Bl6 mice (20-30 g; Charles River) were anesthetized with 1.5% isoflurane and injected intrathecally with capsaicin (10 μg) or vehicle (10% ethanol, 10% Tween 80, saline) in a volume of 5.0 μl with a luer-tipped Hamilton syringe at the level of the pelvic girdle. Behavioral tests were performed 1 to 16 days after capsaicin injection.

Generation of Mrgprd^{DTR} mice

A targeting construct comprised of DTR followed by EMCV-IRES, EGFPf, and a self-excising *loxP*-flanked, neomycin-resistant cassette (ACN) (Bunting et al, 1999) was designed to replace the entire coding region of *Mrgprd*, located within

the second exon. To clone DTR into the ATG initiation site, two separate segments were created by PCR with overlapping oligonucleotide pairs. The overlapping sequences, 5'-ggt tct tct tct acc cat agg aCC ATG GGC ATG AAG CTG CTG CCG TCG GTG G-3', contain the 5' untranslated sequences of *Mrgprd* (50 bps upstream from the ATG initiation codon, small letters) and DTR sequences fused together. The PCR products of the two segments were gel-purified and used as templates for the final PCR using the 5' primer of the first segment and 3' primer of the second segment, which contains the entire coding sequences of DTR. These two primers contain restriction sites allowing for the PCR product to be cloned into the Mrgprd targeting construct as described previously (Zylka et al, 2005). Gene targeting in embryonic stem cells by homologous recombination was performed as described (Zylka et al, 2005)

Histology

Immunohistochemistry (IHC) was performed on spinal cord, DRG and skin as previously described (Lewinter et al, 2004; Zylka et al, 2005; Shields et al, 2007). Antibodies: rabbit anti-GFP (1:1000; Molecular Probes), chicken anti-GFP (1:1000; Aves Labs), goat anti-DTR (1:500; anti-human HB-EGF, R&D), rabbit anti-5HT-1D (1:10,000; gift of A. Ahn, UCSF), rabbit anti-AQP1 (1:10,000; Chemicon Inc.), mouse anti-calbindin (1:5000; Sigma), guinea pig anti-CGRP (1:800; Peninsula), rabbit anti-CGRP (1:100,000; Peninsula), rabbit anti-NK1 receptor (1:4,000; Novus Biologicals), guinea pig anti-TRPV1 (1:5000; DAB or 1:1000; fluorescence; gift of D. Julius, UCSF), rabbit anti-TRPV2 (1:15000; gift of

D. Julius), mouse anti-NeuN (1:1000; Chemicon), and rabbit anti-Fos (1:50000; Oncogene). For fluorescent IB4 binding, we included 1:100 isolectin GS-IB4 (either Alexa Fluor 647 or Alexa Fluor 568 conjugated, Molecular Probes) during the secondary antibodies incubations. For diaminobenzidine-labeled IB4 binding, biotinylated IB4 (1:500; Vector Laboratories) was added instead of primary antibody solution.

Fos expression

Three mice per treatment group were anesthetized with 1.5 g/kg i.p. urethane (Sigma) 20 min prior to immersion of the hindpaw in a 55ºC waterbath, up to the ankle, for 30 s, three times, with a 1 min interstimulus interval. Two hours after the stimulus, mice were perfused, and L4/L5 spinal cord sections were processed for Fos immunohistochemistry. Digitized images of ten randomly selected sections per animal were captured using both brightfield and darkfield illumination. Using the darkfield image as a guide, a line was drawn at the border between the relatively dark substantia gelatinosa (lamina II) and the more lucent or opaque lamina III. Counts of Fos immunoreactive profiles were taken for lamina I/II and V.

Densitometry

Digitized images were captured with a CCD camera (Zeiss Axiocam, Thornwood, NY) attached to a Nikon Eclipse microscope. Image analysis was performed using NIH Image software (http://rsb.info.nih.gov/nih-image). Briefly, the area of

staining was outlined, then pixel density within the selected area was measured and multiplied by the total area selected. Data were collected from five randomly selected sections from at least four animals per treatment group.

Fluorogold injections

One week after capsaicin or vehicle treatment, three animals from each group were used for a Fluorogold (Fluorochrome, LLC, Denver, CO) retrograde tracing study. Animals were anesthetized with a mixture of ketamine and xylazine (60 mg/kg and 8 mg/kg, respectively), a laminectomy was made to expose the L4 or L5 segment of the spinal cord and then the dura was retracted. Three separate 1.0 µl injections of Fluorogold were made in each side of the spinal cord, approximately 1.0 mm apart in the rostro-caudal direction, at a depth of approximately 2.0 mm from the dorsal surface of the spinal cord. A small piece of Gelfoam was soaked in saline and placed over the laminectomy site, then the incision was closed with 6-0 silk suture (Ethicon, Somerville, NJ). Animals were perfused after a survival time of 2 days and DRG tissue was processed for TRPV1 IHC. For cell counts, at least 500 total $NeuN^+$ cells were counted per animal, and the number of $TRPV1^+$ cells was determined as a percentage of $NeuN^+$.

Behavior

All behavioral testing was performed blind to genotype and treatment group during the animals' light period. Wild-type and *Mrgprd*^{DTR} mice were individually

housed at least 1 week before behavioral tests. Where applicable, animals were habituated to the test apparatus for 60 min prior to testing.

von Frey test of mechanical threshold. Mice were placed in plastic chambers on a wire mesh grid and the plantar surface of the hindpaw was stimulated with von Frey filaments (Stoelting Co., Wood Dale, IL or North Coast Medical Inc., Morgan Hill, CA) according to the up-down method (Chaplan et al, 1994).

For response frequency measurements, a series of von Frey filaments of increasing stiffness (0.16, 0.4, 0.6, 1.0, and 1.4 g) were applied. Each filament was applied 10 times with at least a 1 min interval between two consecutive stimuli to the same hindpaw. Results are expressed as the average percentage of withdrawal responses for a given stimulus force value.

Tail immersion test. Tail immersion test was performed as described previously (Lee et al, 2005). Cut-off times were 60 s (at 44^{o}C), and 30 s (at 46, 48, 50 and 52°C) after which the tail was removed from the bath regardless of response.

Hot plate test. For *Mrgprd*^{DTR} mice, animals were placed on a metal plate (IITC Life Science, Woodland Hills, CA) preheated to 48, 50, 52 or 55°C, and latency to hindpaw licking, shaking or jumping was measured as an average of 3 trials per mouse taken ≥ 5 min apart. Cut-off latencies were 80 s (at 48°C), 40 s (at 50°C), and 20 s (at 52 and 55°C).

For capsaicin-treated mice, animals were placed on a hot plate apparatus (Columbus Instruments, Columbus, OH) and latency to lick the hindpaws or jump was recorded as the average of 3 trials per animal taken ≥ 5 min apart. Cut-off latency to avoid tissue damage was 30 s.

Hargreaves (radiant heat) test. Animals were placed in plastic chambers on a glass surface heated to 25ºC through which radiant heat (Dept of Anesthesiology, UC San Diego, La Jolla, CA, or IITC Life Science) was focused on the hindpaw. Latency to withdraw the paw was measured as the average of at least 3 trials per animal taken ≥ 5 min apart. Cut-off latency to avoid tissue damage was 20 s.

Single cold plate. Mice were placed on an aluminum plate cooled to -5ºC. Latency to display a vigorous withdrawal of the hindpaw was measured as the average of 2 trials per animal taken ≥ 5 min apart. Cutoff latency to avoid tissue damage was 1 min.

Temperature preference. A two-plate choice task was used to assess temperature preference. Animals were placed into a plastic chamber whose floor consisted of two identical aluminum plates, the temperature of which could be regulated independently. The time the animal spent on each of the two sides was measured during 5 min. A trial was aborted if the mouse failed to at least touch

both plates within the first minute. To control for possible side preference or room cues, the test was repeated once with the location of the plates switched. Mice were first acclimated to the two-plate apparatus with a trial in which both plates were set to 32ºC (for *Mrgprd*^{DTR} mice) or 30ºC (for capsaicin-treated mice). On subsequent days, the temperature of one plate was set to a range of temperatures from 5-45ºC while the other was held constant at 32 or 30ºC, and time spent on 32/30ºC plate was measured as an average of the two trials.

Complete Freund's Adjuvant (CFA)-induced heat and mechanical hypersensitivity. An intraplantar injection of 20 µl of 100% CFA (Sigma, Fig. 1C, D; 3C, D) or 10 µl of a 1:1 saline/CFA (Fig. 5C, 6B) emulsion was made through a 30 gauge needle. Heat and mechanical thresholds were measured using the hindpaw radiant heat and von Frey tests, as described above, beginning 24 hours after the injection and then daily for one week.

Statistical analysis

Behavioral, densitometry, and Fos data were analyzed by Student's t-test, one- and two-way repeated measures ANOVA (Bonferroni post-test) or Mann-Whitney U test, with $p<0.05$ considered to be significant.

References

Abrahamsen B, Zhao J, Asante CO, Cendan CM, Marsh S, Martinez-Barbera JP, Nassar MA, Dickenson AH, Wood JN (2008) The cell and molecular basis of mechanical, cold, and inflammatory pain. *Science* 321:702-705.

Bautista DM, Siemens J, Glazer JM, Tsuruda PR, Basbaum AI, Stucky CL, Jordt SE, Julius D (2007) The menthol receptor TRPM8 is the principal detector of environmental cold. *Nature* 448:204-208.

Bautista DM, Jordt SE, Nikai T, Tsuruda PR, Read AJ, Poblete J, Yamoah EN, Basbaum AI, Julius D (2006) TRPA1 mediates the inflammatory actions of environmental irritants and proalgesic agents. *Cell* 124:1269-1282.

Binshtok AM, Bean BP, Woolf CJ (2007) Inhibition of nociceptors by TRPV1-mediated entry of impermeant sodium channel blockers. *Nature* 449:607-610.

Braz JM, Nassar MA, Wood JN, Basbaum AI (2005) Parallel "pain" pathways arise from subpopulations of primary afferent nociceptor. *Neuron* 47:787-793.

Bunting M, Bernstein KE, Greer JM, Capecchi MR, THomas KR (1999) Targeting genes for self-excision in the germ line. *Genes Dev* 13:1524-1528.

Cain DM, Khasabov SG, Simone DA (2001) Response properties of mechanoreceptors and nociceptors in mouse glabrous skin: an in vivo study. *J Neurophysiol* 85:1561-1574.

Caterina MJ (2003) Vanilloid receptors take a TRP beyond the sensory afferent. *Pain* 105:5-9.

Caterina MJ, Julius D (2001) The vanilloid receptor: a molecular gateway to the pain pathway. *Annu Rev Neurosci* 24:487-517.

Caterina MJ, Rosen TA, Tominaga M, Brake AJ, Julius D (1999) A capsaicin-receptor homologue with a high threshold for noxious heat. *Nature* 398:436-441.

Caterina MJ, Schumacher MA, Tominaga M, Rosen TA, Levine JD, Julius D (1997) The capsaicin receptor: a heat-activated ion channel in the pain pathway. *Nature* 389:816-824.

Caterina MJ, Leffler A, Malmberg AB, Martin WJ, Trafton J, Petersen-Zeitz KR, Koltzenburg M, Basbaum AI, Julius D (2000) Impaired nociception and pain sensation in mice lacking the capsaicin receptor. *Science* 288:306-313.

Chandrashekar J, Hoon MA, Ryba NJ, Zuker CS (2006) The receptors and cells for mammalian taste. *Nature* 444:288-294.

Chaplan SR, Bach FW, Pogrel JW, Chung JM, Yaksh TL (1994) Quantitative assessment of tactile allodynia in the rat paw. *J Neurosci Methods* 53:55-63.

Davis JB, Gray J, Gunthorpe MJ, Hatcher JP, Davey PT, Overend P, Harries MH, Latcham J, Clapham C, Atkinson K, Hughes SA, Rance K, Grau E, Harper AJ, Pugh PL, Rogers DC, Bingham S, Randall A, Sheardown SA

(2000) Vanilloid receptor-1 is essential for inflammatory thermal hyperalgesia. *Nature* 405:183-187.

Dong X, Han S, Zylka MJ, Simon MI, Anderson DJ (2001) A diverse family of GPCRs expressed in specific subsets of nociceptive sensory neurons. *Cell* 106:619-632.

Dussor G, Zylka MJ, Anderson DJ and McCleskey EW (2008) Cutaneous sensory neurons expressing the Mrgprd receptor sense extracellular ATP and are putative nociceptors. *J Neurophysiol* 99:1581-9.

Fitzgerald M, Woolf CJ (1982) The time course and specificity of the changes in the behavioural and dorsal horn cell responses to noxious stimuli following peripheral nerve capsaicin treatment in the rat. *Neuroscience* 7:2051-2056.

Gamse R (1982) Capsaicin and nociception in the rat and mouse. Possible role of substance P. *Naunyn Schmiedebergs Arch Pharmacol* 320:205-216.

Holzer P (1991) Capsaicin: cellular targets, mechanisms of action, and selectivity for thin sensory neurons. *Pharmacol Rev* 43:143-201.

Julius D, Basbaum AI (2001) Molecular mechanisms of nociception. *Nature* 413:203-210.

Karai L, Brown DC, Mannes AJ, Connelly ST, Brown J, Gandal M, Wellisch OM, Neubert JK, Olah Z, Iadarola MJ (2004) Deletion of vanilloid receptor 1-expressing primary afferent neurons for pain control. *J Clin Invest* 113:1344-1352.

Lawson JJ, McIlwrath SL, Woodbury CJ, Davis BM, Koerber HR (2008) TRPV1 unlike TRPV2 is restricted to a subset of mechanically insensitive cutaneous nociceptors responding to heat. *J Pain* 9:298-308.

Lee H, Iida T, Mizuno A, Suzuki M, Caterina MJ (2005) Altered thermal selection behavior in mice lacking transient receptor potential vanilloid 4. *J Neurosci* 25:1304-1310.

Lewinter RD, Skinner K, Julius D, Basbaum AI (2004) Immunoreactive TRPV-2 (VRL-1), a capsaicin receptor homolog, in the spinal cord of the rat. *J Comp Neurol* 470:400-408.

Luquet S, Perez FA, Hnasko TS, Palmiter RD (2005) NPY/AgRP neurons are essential for feeding in adult mice but can be ablated in neonates. *Science* 310:683-685.

Melzack R, Wall PD (1962) On the nature of cutaneous sensory mechanisms. *Brain* 85:331-356.

Molliver DC, Snider WD (1997) Nerve growth factor receptor TrkA is down-regulated during postnatal development by a subset of dorsal root ganglion neurons. *J Comp Neurol* 381:428-438.

Perl ER (1996) Cutaneous polymodal receptors: characteristics and plasticity. *Progress Brain Res* 113:21-37.

Perl ER (2007) Ideas about pain, a historical view. *Nat Rev Neurosci* 8:71-80.

Potrebic S, Ahn AH, Skinner K, Fields HL, Basbaum AI (2003) Peptidergic nociceptors of both trigeminal and dorsal root ganglia express serotonin

1D receptors: implications for the selective antimigraine action of triptans. *J Neurosci* 23:10988-10997.

Price TJ, Flores CM (2007) Critical evaluation of the colocalization between calcitonin gene-related peptide, substance P, transient receptor potential vanilloid subfamily type 1 immunoreactivities, and isolectin B4 binding in primary afferent neurons of the rat and mouse. *J Pain* 8:263-272.

Saito M, Iwawaki T, Taya C, Yonekawa H, Noda M, Inui Y, Mekada E, Kimata Y, Tsuru A, Kohno K (2001) Diphtheria toxin receptor-mediated conditional and targeted cell ablation in transgenic mice. *Nat Biotech* 19:746-750.

Scott K (2005) Taste recognition: food for thought. *Neuron* 48:455-464.

Shields SD, Mazario J, Skinner K, Basbaum AI (2007) Anatomical and functional analysis of aquaporin 1, a water channel in primary afferent neurons. *Pain* 131:8-20.

Snider WD, McMahon SB (1998) Tackling pain at the source: new ideas about nociceptors. *Neuron* 20:629-632.

Story GM, Peier AM, Reeve AJ, Eid SR, Mosbacher J, Hricik TR, Earley TJ, Hergarden AC, Andersson DA, Hwang SW, McIntyre P, Jegla T, Bevan S, Patapoutian A (2003) ANKTM1, a TRP-like channel expressed in nociceptive neurons, is activated by cold temperatures. *Cell* 112:819-829.

Stucky CL, Lewin GR (1999) Isolectin B(4)-positive and -negative nociceptors are functionally distinct. *J Neurosci* 19:6497-6505.

Tarpley JW, Kohler MG, Martin WJ (2004) The behavioral and neuroanatomical effects of IB4-saporin treatment in rat models of nociceptive and neuropathic pain. *Brain Res* 1029:65-76.

Vulchanova L, Olson TH, Stone LS, Riedl MS, Elde R, Honda CN (2001) Cytotoxic targeting of isolectin IB4-binding sensory neurons. *Neuroscience* 108:143-155.

Yaksh TL, Farb DH, Leeman SE, Jessell TM (1979) Intrathecal capsaicin depletes substance P in the rat spinal cord and produces prolonged thermal analgesia. *Science* 206:481-483.

Zylka MJ, Rice FL, Anderson DJ (2005) Topographically distinct epidermal nociceptive circuits revealed by axonal tracers targeted to Mrgprd. *Neuron* 45:17-25.

Zylka MJ, Dong X, Southwell AL, Anderson DJ (2003) Atypical expansion in mice of the sensory neuron-specific Mrg G protein-coupled receptor family. *Proc Natl Acad Sci U S A* 100:10043-10048.

Figure 1. Specific ablation of Mrgprd^{+} neurons in mice.

(A) Mrgprd^{DTR} targeting construct.

(B-D) DTR expression in the absence of DTX does not impair the survival of Mrgprd^{+} neurons, determined using an independent, EGFPf-expressing allele in *Mrgprd$^{EGFPf/DTR}$* trans-heterozygous mice.

(E-N) Sections of the DRG (E-H), spinal cord (I-L), and glabrous skin (M-N) from DTX-treated *Mrgprd$^{EGFPf/+}$* (E,G,I,K,M) and *Mrgprd$^{EGFPf/DTR}$* mice. (F,H,J,L,N) were stained for the indicated markers. Note selective loss of Mrgprd^{+} cells (green) and fibers (F, H, J, L, N). See Supplemental Table I for quantification. Scale bars in D, F, H, J, L = 50 μm, 25 μm in N.

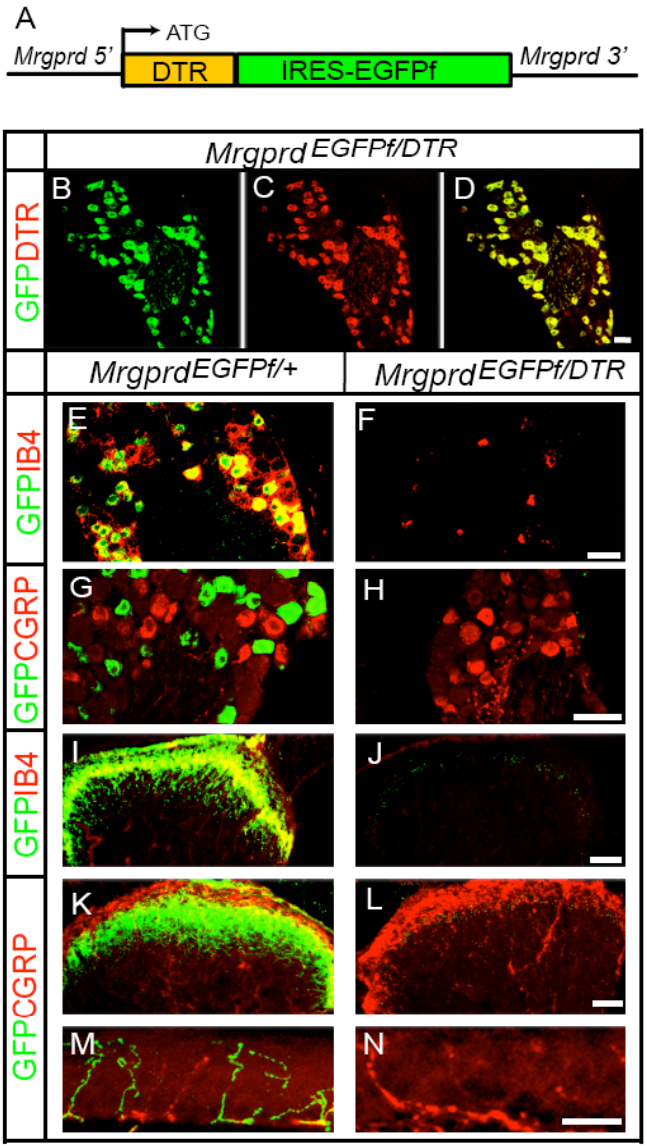
A
ATG
Mrgprd 5'
DTR
IRES-EGFPf
Mrgprd 3'
Mrgprd EGFPf/DTR
GFPDTR
B
C
D
Mrgprd EGFPf/+
Mrgprd EGFPf/DTR
GFPIB4
E
F
GFPCGRP
G
H
GFPIB4
I
J
GFPCGRP
K
L
M
N

Figure 2. Mice lacking Mrgprd^{+} neurons exhibit selective deficits in mechanosensitivity.

(A) Mechanical thresholds determined with von Frey test, before and after DTX injection. (*p<.05, **p<.01, Student's t test).

(B) von Frey test prior to (BL) and post-CFA (**p<.01, ***p<.001, two-way ANOVA with Bonferroni post-tests).

(C) Normalized mechanical threshold at post-CFA day 1 relative to pre-CFA baseline (*p<.05, Mann-Whitney U-Test).

(D) Tail immersion test.

(E) Hot plate test. The 55^{o}C data used a separate cohort of mice.

(F) Radiant heat test, prior to (BL) and post-CFA. Data represent means ± SEM; n=6-10 for all tests.

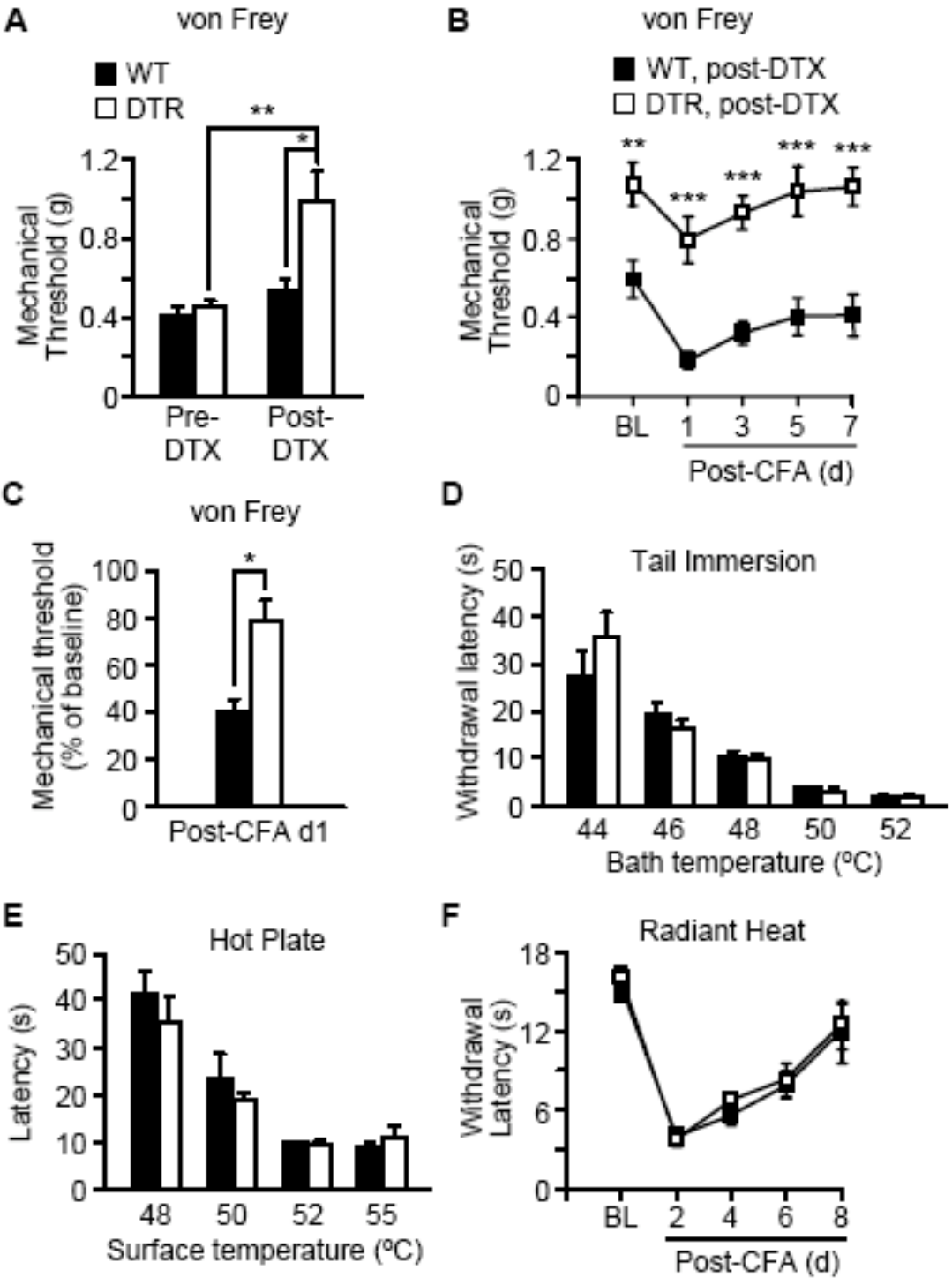
A
von Frey
WT
DTR
**
*
Mechanical Threshold (g)
1.2
0.8
0.4
0
Pre-DTX
Post-DTX
B
von Frey
WT, post-DTX
DTR, post-DTX
**
***
***
***
***
Mechanical Threshold (g)
1.2
0.8
0.4
0
BL
1
3
5
7
Post-CFA (d)
C
von Frey
*
Mechanical threshold (% of baseline)
100
80
60
40
20
0
Post-CFA d1
D
Tail Immersion
Withdrawal latency (s)
50
40
30
20
10
0
44
46
48
50
52
Bath temperature (ºC)
E
Hot Plate
Latency (s)
50
40
30
20
10
0
48
50
52
55
Surface temperature (ºC)
F
Radiant Heat
Withdrawal Latency (s)
18
12
6
0
BL
2
4
6
8
Post-CFA (d)

Figure 3. Intrathecal capsaicin treatment selectively ablates the central terminals of TRPV1$^+$ nociceptors.

(A-D) Immunostaining in lumbar dorsal horn 16d after intrathecal vehicle- (left) or capsaicin (right). Staining for (A) TRPV1, and (B) CGRP was significantly reduced by capsaicin. Staining for IB4 (C); and TRPV2 (D) was unchanged.

(E) Density of staining: mean ± SEM; *p<.0005, Student's t test. For TRPV1 staining, n=8 for capsaicin-treated, n=10 for vehicle-treated, and n=4 per group for all others.

(F) Double labeling for TRPV1 (red) and Mrgprd-GFP (green) in vehicle- (left) and capsaicin-treated (right) mice. Scale bar = 200 μm.

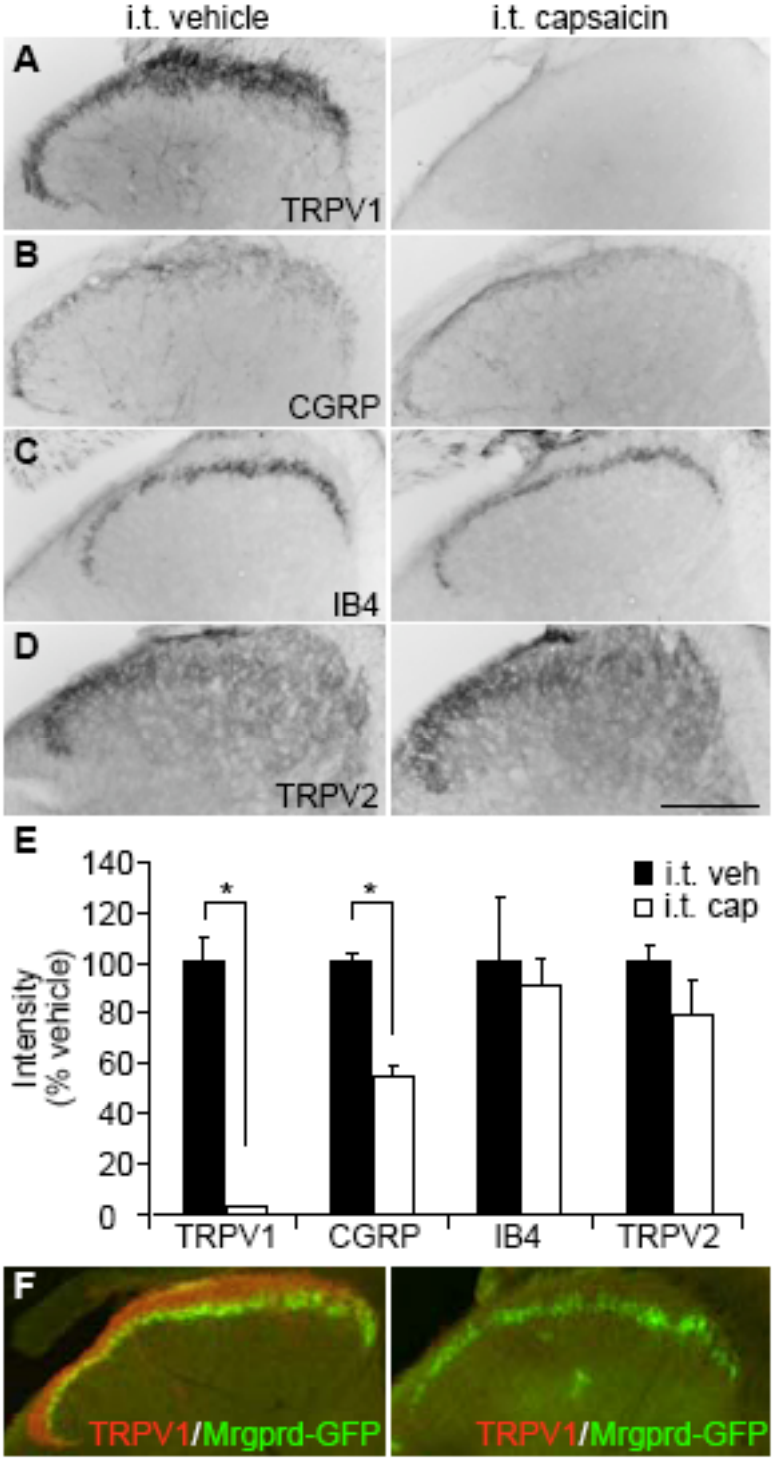
i.t. vehicle
i.t. capsaicin
A
TRPV1
B
CGRP
C
IB4
D
TRPV2
E
Intensity (% vehicle)
140
120
100
80
60
40
20
0
*
*
i.t. veh
i.t. cap
TRPV1
CGRP
IB4
TRPV2
F
TRPV1/Mrgprd-GFP
TRPV1/Mrgprd-GFP

Figure 4. Capsaicin-treated mice exhibit a complete and selective loss of heat pain sensitivity.

(A) Latency to lick/jump on 55^{o}C hot plate, 1d after intrathecal capsaicin or vehicle (^*p*<.0001, Student's t test), and (B) at weekly intervals after capsaicin (n=4).

(C) CFA-induced heat hypersensitivity (**p<.01, ^p<.0001, two-way rmANOVA with Bonferroni).

(D) Temperature preference assay (**p<.01, Student's t test).

(E) Fos induced by hindpaw immersion in 55^{o}C waterbath.

(F) Fos^{+} neurons in laminae I/II and V per 40μm section (**p<.01, Student's t test; n=3 per group).

(G) Mechanical threshold (von Frey).

(H) CFA-induced mechanical hypersensitivity, ^p<.0001, two-way rmANOVA with Bonferroni). Data represent means ± SEM. Unless otherwise noted, n=8-10.

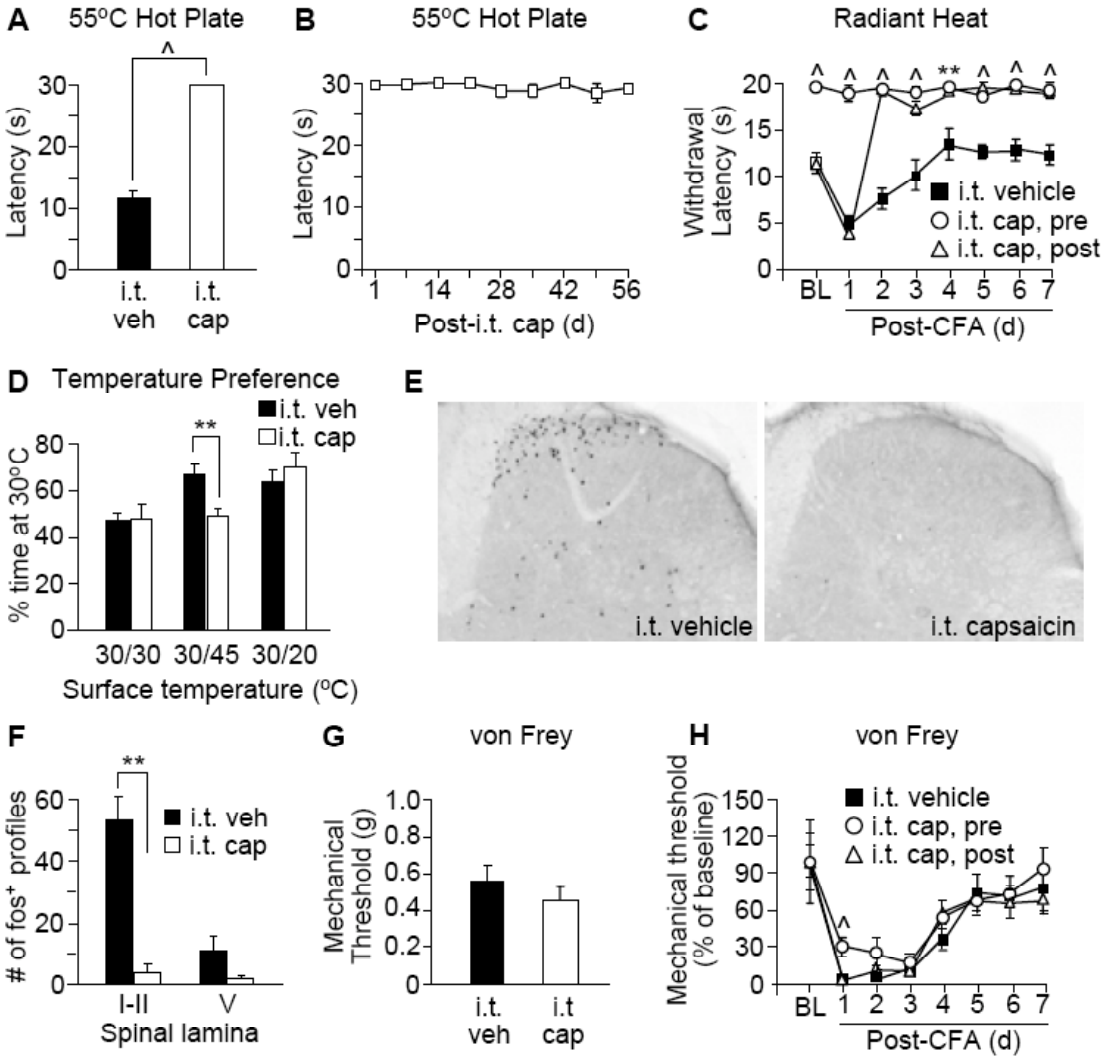
A
55°C Hot Plate
Latency (s)
i.t. veh
i.t. cap
B
55°C Hot Plate
Latency (s)
Post-i.t. cap (d)
C
Radiant Heat
Withdrawal Latency (s)
i.t. vehicle
i.t. cap, pre
i.t. cap, post
BL
Post-CFA (d)
D
Temperature Preference
i.t. veh
i.t. cap
% time at 30°C
30/30 30/45 30/20
Surface temperature (°C)
E
i.t. vehicle
i.t. capsaicin
F
# of fos+ profiles
i.t. veh
i.t. cap
I-II
V
Spinal lamina
G
von Frey
Mechanical Threshold (g)
i.t. veh
i.t cap
H
von Frey
Mechanical threshold (% of baseline)
i.t. vehicle
i.t. cap, pre
i.t. cap, post
BL
Post-CFA (d)

Figure 5. TRPV1$^+$ neurons do not contribute to residual mechanical pain sensitivity in mice lacking Mrgprd$^+$ neurons.

(A) Mechanical (von Frey) and (B) heat (radiant heat) responsiveness in DTX-treated WT or *Mrgprd*^{DTR} mice, before and after intrathecal capsaicin (n=3 for WT/DTX and n=6 for *Mrgprd*^{DTR}/DTX; ***p*<.001, ****p*<.0001, n.s., not significant, Student's t test).

(C) Schematic illustrating modality-specific contributions of Mrgprd$^+$ and TRPV1$^+$ fibers to behavior and their termination zones in the epidermis and spinal cord [14]. The second-order targets of Mrgprd$^+$ afferents are shown projecting to deeper laminae, before engaging ascending pathways [1] SG, stratum granulosum; SS, stratum spinosum. I, lamina I; IIo, lamina II outer; IIi, lamina II inner.

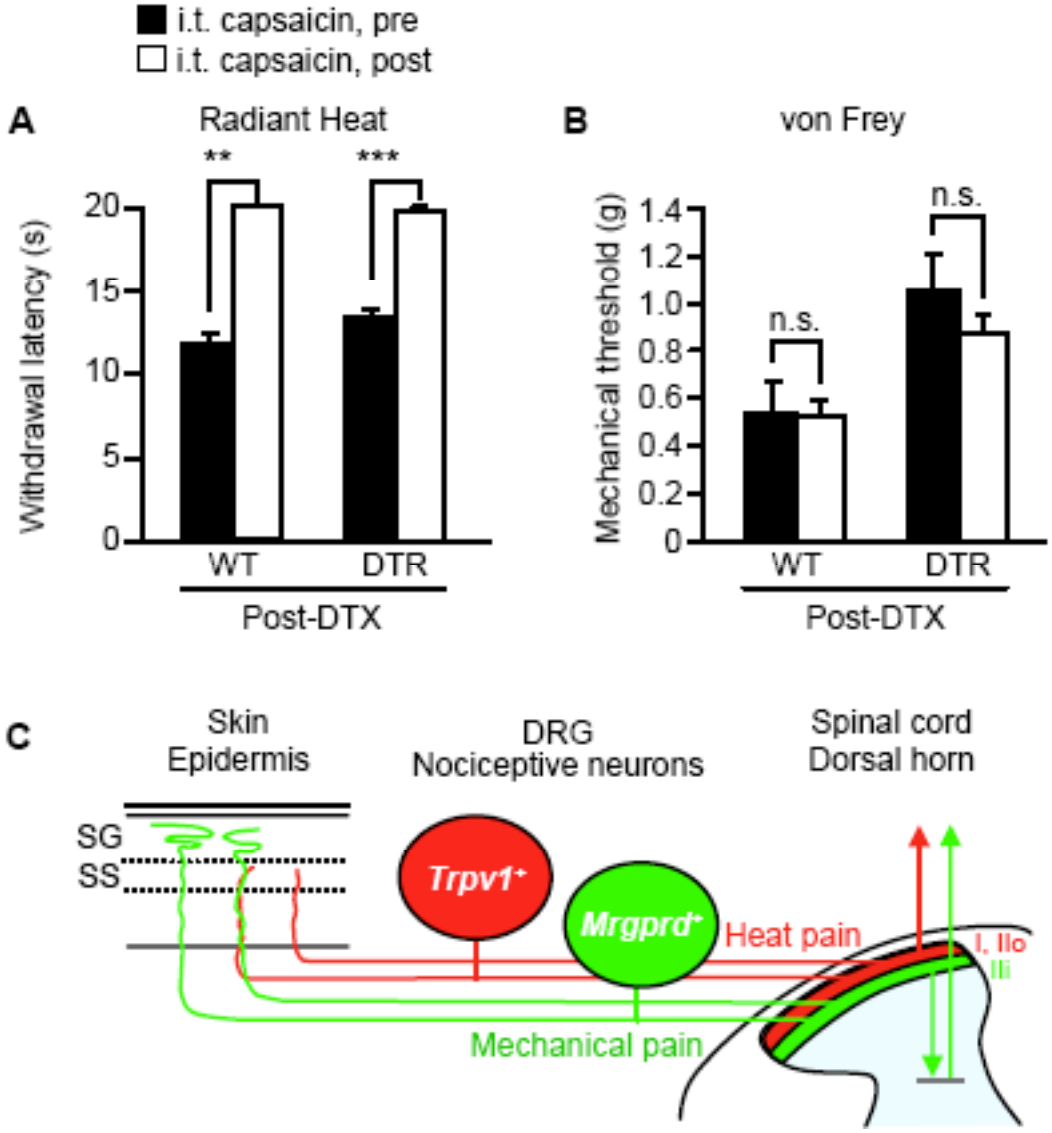
i.t. capsaicin, pre
i.t. capsaicin, post
A
Radiant Heat
**
***
Withdrawal latency (s)
20
15
10
5
0
WT
DTR
Post-DTX
B
von Frey
n.s.
n.s.
Mechanical threshold (g)
1.4
1.2
1.0
0.8
0.6
0.4
0.2
0
WT
DTR
Post-DTX
C
Skin
Epidermis
DRG
Nociceptive neurons
Spinal cord
Dorsal horn
SG
SS
Trpv1+
Mrgprd+
Heat pain
Mechanical pain
I, IIo
IIi

Supplemental Figure and Table Legends

Supplemental Figure S1. Mice lacking Mrgprd^{+} neurons exhibit deficits in mechanosensitivity.

Paw withdrawal frequency to von Frey filaments post-DTX (n=8 per genotype; *p<.05, **p<.01, two-way ANOVA with Bonferroni post-tests). Data represent means±SEM.

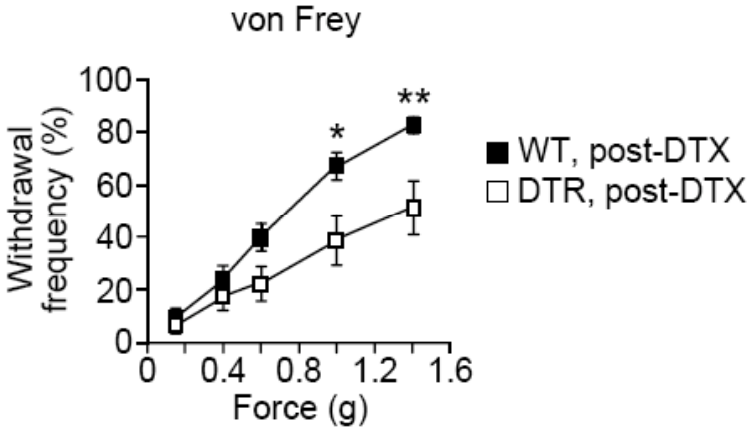
von Frey
Withdrawal frequency (%)
100
80
60
40
20
0
0
0.4
0.8
1.2
1.6
Force (g)
*
**
WT, post-DTX
DTR, post-DTX

Supplemental Figure S2. Mrgprd^{+} neurons were selectively ablated in *Mrgprd^{DTA}* mice.

(A) The targeting construct was designed to express diphtheria toxin A fragment (DTA) in Mrgprd^{+} cells in the presence of doxycycline. However, *Mrgprd^{DTA}* mice expressed DTA in a doxycycline-independent manner, causing an ablation of Mrgprd^{+} neurons from birth.

(B) *in situ* hybridization was performed with a Mrgprd antisense riboprobe on adult DRG sections from wild-type and *Mrgprd^{DTA}* mice.

(C) The total number of GFP^{+} and CGRP^{+} L5 DRG neurons in wild-type and *Mrgprd^{DTA}* mice (n=1 each). Note selective and complete loss of Mrgprd^{+} cell bodies.

(D-G) Sections of the glabrous skin (D,F), and spinal cord (E,G) from *Mrgprd$^{EGFPf/+}$* (D,E) and *Mrgprd$^{EGFPf/DTA}$* mice (F,G) were stained for the indicated markers. Note selective loss of Mrgprd^{+} fibers (F,G, green).

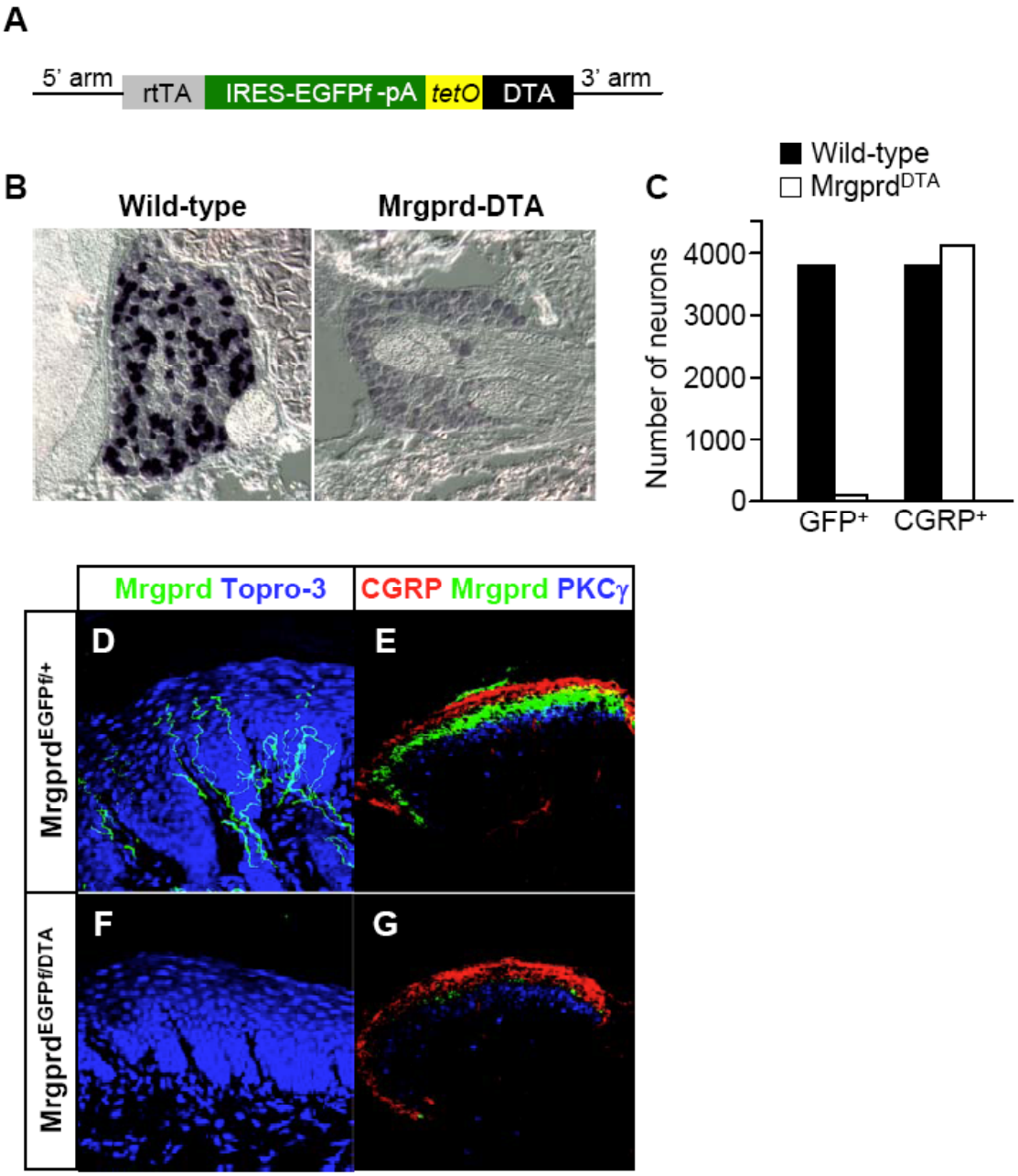
A
5' arm
rtTA
IRES-EGFPf -pA
tetO
DTA
3' arm
B
Wild-type
Mrgprd-DTA
C
Wild-type
MrgprdDTA
Number of neurons
4000
3000
2000
1000
0
GFP+
CGRP+
Mrgprd Topro-3
CGRP Mrgprd PKCγ
D
E
F
G
MrgprdEGFPf/+
MrgprdEGFPf/DTA

Supplemental Figure S3. Mice lacking Mrgprd^{+} neurons from birth exhibit normal mechanical and thermal sensitivity.

(A) von Frey

(B) hot plate

(C) radiant heat test. n=9 for wild-type and n=8 for *Mrgprd*^{DTA} ("DTA") mice. Data represent means±SEM.

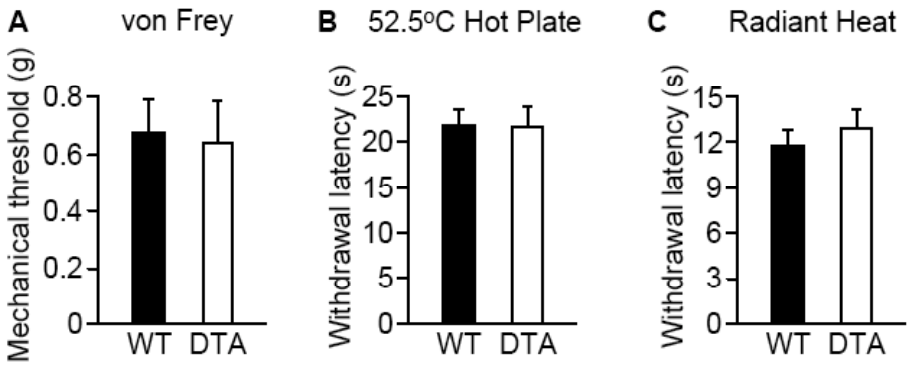
A
von Frey
Mechanical threshold (g)
0.8
0.6
0.4
0.2
0
WT
DTA
B
52.5°C Hot Plate
Withdrawal latency (s)
25
20
15
10
5
0
WT
DTA
C
Radiant Heat
Withdrawal latency (s)
15
12
9
6
3
0
WT
DTA

Supplemental Figure S4. Mice lacking Mrgprd^{+} neurons and capsaicin-treated mice exhibit normal cold sensitivity.

(A) Percentage of time spent at 32^{o}C during a 5 min test period when given a choice between two temperatures (32 vs. 32, 32 vs. 20, 32 vs. 10, 32 vs. 5^{o}C; n=10 for all groups).

(B and C) Paw withdrawal latency on a -5^{o}C plate (n=11 for WT/DTX vs. n=9 for *Mrgprd*^{DTR}/DTX and n=10 for i.t. vehicle vs. n=8 for i.t. capsaicin). Data represent means±SEM.

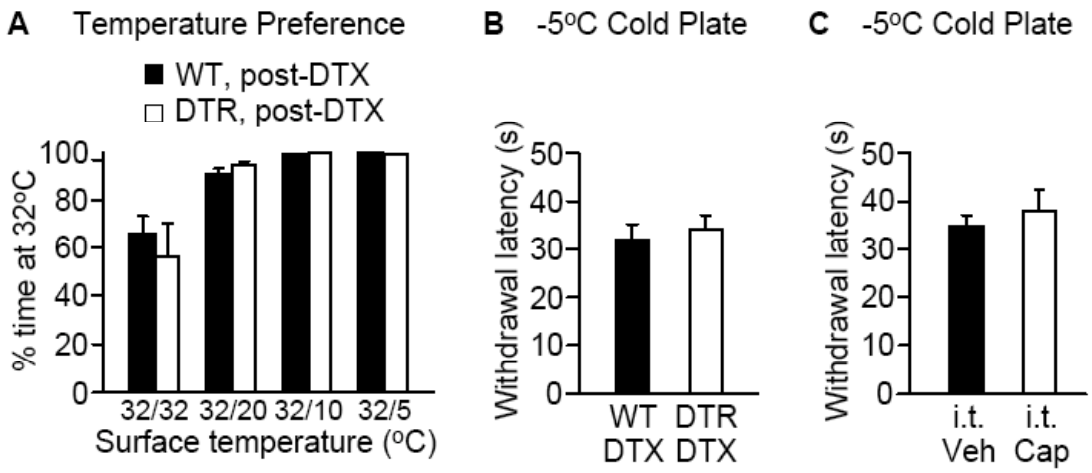
A Temperature Preference
WT, post-DTX
DTR, post-DTX
% time at 32°C
100
80
60
40
20
0
32/32 32/20 32/10 32/5
Surface temperature (°C)
B -5°C Cold Plate
Withdrawal latency (s)
50
40
30
20
10
0
WT DTX
DTR DTX
C -5°C Cold Plate
Withdrawal latency (s)
50
40
30
20
10
0
i.t. Veh
i.t. Cap

Supplemental Figure S5. Intrathecal capsaicin destroys the central terminals, but not the DRG cell bodies, of $TRPV1^+$ afferents. One week after intrathecal capsaicin or vehicle, mice received a lumbar spinal injection of the retrograde tracer, fluorogold.

(A) In L4 or L5 DRG of vehicle-treated mice, the vast majority of $TRPV1^+$ cells (middle) contain fluorogold (left).

(B) In capsaicin-treated mice, very few $TRPV1^+$ cells (middle) contain fluorogold (left). Right panels show merged images.

(C) % of $TRPV1^+$ cells that contain fluorogold.

(D) $TRPV1^+$ DRG neurons, expressed as a percentage of $NeuN^+$ cells, demonstrating that capsaicin treatment did not alter TRPV1 staining of DRG cell bodies. Data presented as mean±SEM; ***p<.0001, Student's t test; n=3 for all.

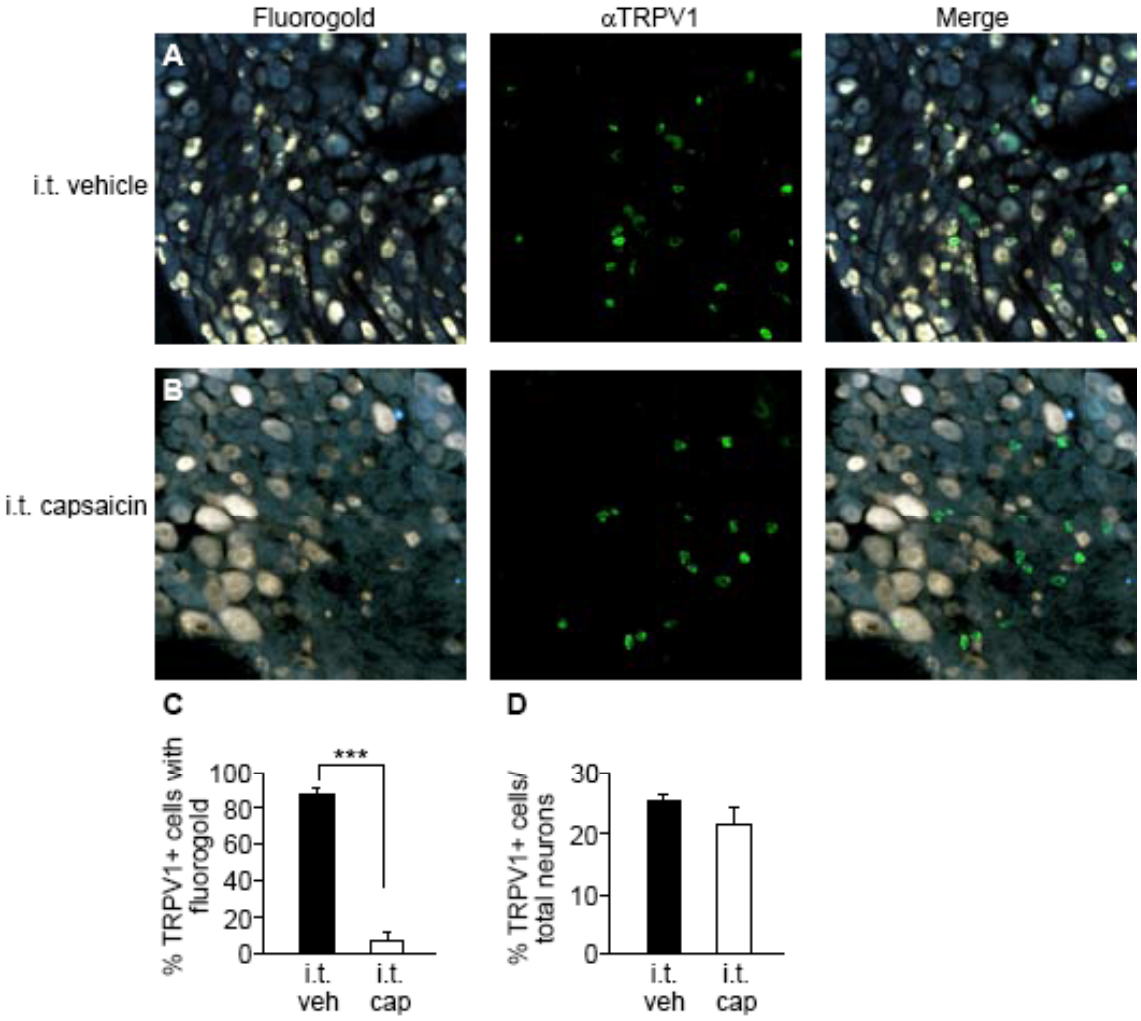
Fluorogold
αTRPV1
Merge
A
i.t. vehicle
B
i.t. capsaicin
C
% TRPV1+ cells with fluorogold
100
80
60
40
20
0
***
i.t. veh
i.t. cap
D
% TRPV1+ cells/ total neurons
30
20
10
0
i.t. veh
i.t. cap

Supplemental Figure S6. Intrathecal capsaicin selectively reduces immunostaining for markers of TRPV1$^+$ afferents.

Immunostaining of lumbar dorsal horn 16d after intrathecal vehicle- (left) or capsaicin (right).

(A) 5HT-1D receptor and (B) aquaporin-1 (AQP1) immunoreactivity were significantly reduced by capsaicin. Note that staining for AQP1, which is found in both TRPV1$^+$ and TRPV1$^-$ nociceptors, was depleted in laminae I and outer II (arrowheads), namely in the region targeted by the TRPV1$^+$ afferents, but not in inner lamina II, which is targeted by Mrgprd$^+$ afferents.

Staining for (C) calbindin and (D) substance P receptor (NK1), did not change. (E) Density of staining for the different markers; mean±SEM; *p<.005, Student's t test; for NK1 staining, n=6 per group, and n=4 per group for all others. Scale bar = 200 μm.

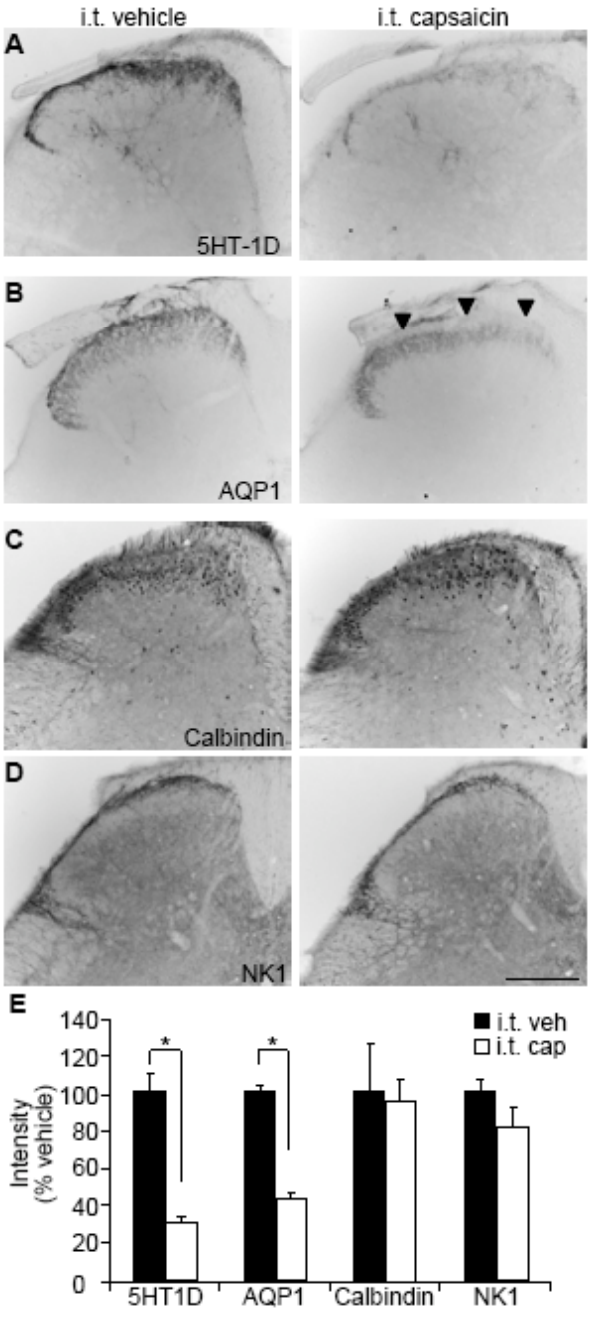
i.t. vehicle
i.t. capsaicin
A
5HT-1D
B
AQP1
C
Calbindin
D
NK1
E
i.t. veh
i.t. cap
Intensity (% vehicle)
140
120
100
80
60
40
20
0
*
*
5HT1D
AQP1
Calbindin
NK1

Supplemental Table 1. DTX injection in adult *Mrgprd*^{DTR} mice eliminates IB4^{+} but not CGRP^{+} DRG neurons. 5 control (*Mrgprd*^{EGFPf}) and 4 *Mrgprd*^{DTR} mice, aged 8-10 weeks old, were injected with DTX (100 μg/kg) at day 1 and day 4, then killed between two to four weeks after the second injection. At least 4 to 9 DRG from each perfused animal were collected and sectioned. After triple labeling with either IB4, GFP and NeuN, or CGRP, GFP, and NeuN, sections from the different genotypes were imaged by confocal fluorescence microscopy using the same gain settings. Marker positive cells were counted in the different color channels using Photoshop. The percentages of IB4^{+}, Mrgprd^{+} (GFP^{+}), or CGRP^{+} neurons were determined by dividing the total number of marker^{+} cells by the total number of NeuN^{+} cells in each section. Ten to twenty sections were counted for each marker for each animal. Data represent means±SD. *Mrgprd*^{DTR} mice without DTX injection have a similar % of IB4^{+} or CGRP^{+} neurons as control mice injected with DTX (data not shown). About 4.9±2.8% of CGRP^{+} neurons are also GFP^{+} and about 3.8±1.7% of GFP^{+} neurons are also CGRP^{+}. On average, about 1.2±0.7% NeuN^{+} cells are double-positive for CGRP and GFP.

[a]Pairwise comparison on the same sections double-stained for IB4 and Mrgprd.

[b]Pairwise comparison on the same sections double-stained for CGRP and Mrgprd.

*p<.0001 between same marker expressed in animals with different genotype.

"Expected CGRP$^+$ neurons" indicates the predicted percentage of CGRP/NeuN$^+$ neurons, assuming that all Mrgprd$^+$ neurons, and only those neurons, are ablated. The number obtained (39.9% CGRP$^+$ neurons) is similar to the measured % of CGRP$^+$ neurons (41%) after DTX administration. We conclude that there is no significant reduction in the CGRP population after DTX administration.

	$Mrgprd^{EGFPf/+}$	$Mrgprd^{EGFPf/DTR}$
% $IB4^+$ neurons[a]	33.5±1.5%	5.9±0.5%*
% $Mrgprd^+$ neurons[a]	29.4±2.6%	0.5±0.5%*
% $CGRP^+$ neurons[b]	27.4±3.5%	41.0±7.4%*
% $Mrgprd^+$ neurons[b]	31.3±3.7%	0.4±0.5%*
% $CGRP^+$ neurons (predicted)		39.9%

Conclusion

Multiple, molecularly and anatomically distinct nociceptor populations exist, however, the functional relevance of these anatomical distinctions has remained unclear, as electrophysiological studies have failed to detect substantial differences between the nociceptor subtypes. Here, we have used genetic and pharmacological approaches to further our understanding of the anatomical and functional segregation of nociceptor populations. We created a line of knock-in mice to show that expression of the heat and capsaicin receptor, TRPV1, is largely limited to the peptidergic class of primary afferent nociceptors. We additionally demonstrate that $TRPV1^+$ nociceptors make a critical and specific contribution to the behavioral response to noxious heat stimuli, while $Mrgprd^+$ neurons selectively contribute to behavioral responses to noxious mechanical stimuli.

These findings show that noxious modality discrimination begins at the earliest stages of sensory processing. Consistent with this idea, a recent report from our lab detailed the segregation of opioid receptors in different populations of primary afferent neurons, with the mu opioid receptor (MOR) being expressed by the peptidergic class of nociceptors, and the delta opioid receptor (DOR) being expressed by a subset of Aδ myelinated neurons, as well as by a large percentage of nonpeptidergic nociceptors (many of which are $Mrgprd^+$) (Scherrer et al, 2009). Furthermore, intrathecal injection of selective agonists for the MOR

or the DOR led to a specific analgesia to noxious heat or mechanical stimuli, but not to both. Thus, the effect of subtype-specific neuronal ablation is mimicked by transiently silencing nociceptor subtypes using pharmacological methods.

Intriguingly, these data suggest the possibility that labeled lines of modality specific information are maintained in the spinal cord and brain. This is further suggested by genetic tracing studies that showed that the peptidergic and nonpeptidergic subtypes access different brain areas through distinct ascending circuits (Braz et al, 2005). Modality-specific spinal cord circuits are also implied by the fact that MOR and DOR agonists caused modality-specific analgesia, as these receptors are present on post-synaptic spinal cord neurons, in addition to being expressed by primary afferent terminals (Scherrer et al, 2009). If these spinal cord neurons received convergent information from afferents that signal multiple modalities, then injection of MOR and DOR agonists would be expected to generate analgesia to multiple modalities of noxious stimulation.

Genetic tracing studies along with electrophysiological recordings from spinal cord neurons will be important in determining the degree of convergence versus segregation of nociceptive information in spinal cord circuits. As we have shown that TRPV1 is a selective marker of the heat-sensitive, peptidergic class of nociceptors, this molecule can be used to genetically mark this subset. We are in the process of creating a knock-in mouse line in which Cre recombinase is expressed in $TRPV1^{+}$ neurons. Crossing this mouse with the ZW line, in which

the trans-synaptic tracer wheat germ agglutinin (WGA) is expressed in a Cre-dependent manner (Braz et al, 2005), will allow us to trace peptidergic circuits into the spinal cord and brain. A prediction of the labeled line hypothesis is that the peptidergic population should preferentially synapse onto MOR^+ spinal cord neurons, and should not synapse onto DOR^+ spinal cord neurons. We can additionally test the degree of modality convergence in the spinal cord by making electrophysiological recordings from MOR and DOR^+ spinal cord neurons during heat and mechanical stimulation of the paw, and by recording from spinal cord neurons in the presence or absence of the $TRPV1^+$ or $Mrgprd^+$ subsets of nociceptors. Finally, the development of better genetic tools that allow us to trace circuits across multiple synapses will allow us to determine whether an anatomical substrate exists for the segregation of modality-specific information in downstream CNS regions.

References

Braz JM, Nassar MA, Wood JN, Basbaum AI (2005) Parallel "pain" pathways arise from subpopulations of primary afferent nociceptor. *Neuron* 47:787-93.

Scherrer G, Imamachi N, Cao YQ, Contet C, Mennicken F, O'Donnell D, Kieffer BL, Basbaum AI (2009) Dissociation of the opioid receptor mechanisms that control mechanical and heat pain. *Cell* 137:1148-59.

Publishing Agreement

It is the policy of the University to encourage the distribution of all theses, dissertations, manuscripts. Copies of all UCSF theses, dissertations, and manuscripts will library via the Graduate Division. The library will make all theses, dissertations, manuscripts accessible to the public and will preserve these to the best of their perpetuity.

Please sign the following statement:

I hereby grant permission to the Graduate Division of the University of California, Francisco to release copies of my thesis, dissertation, or manuscript to the Campus provide access and preservation, in whole or in part, in perpetuity.

Daniel Cavanagh 9/12/09

Author Signature Date